Title
CAVITY DESIGN DATA FOR HIGH ENERGY LINEAR ACCELERATORS

Authors
Kitchen, S.W.
Schelberg, A. D.
Hill, B. V.
et al.

Publication Date
1952-12-09

UCRL- 2046

CONFIDENTIAL
SECURITY INFORMATION

DECLASSIFIED

UNIVERSITY OF CALIFORNIA — BERKELEY

RADIATION LABORATORY

CONFIDENTIAL
SECURITY INFORMATION

UNIVERSITY OF CALIFORNIA
Radiation Laboratory

Cover Sheet
Do not remove

INDEX NO. UCRL-2046
This document contains 47 pages
This is copy 10 of 10 series E

DECLASSIFIED

Issued to Information Division

~~CONFIDENTIAL~~
Classification

Each person who receives this document must sign the cover sheet in the space below.

Route to	Noted by	Date	Route to	Noted by	Date

I-5(M)

UCRL-2046

Particle Accelerators and High-Voltage Machines

UNIVERSITY OF CALIFORNIA
Radiation Laboratory

Contract No. W-7405-eng-48

CAVITY DESIGN DATA FOR HIGH ENERGY LINEAR ACCELERATORS

S. W. Kitchen, A. D. Schelberg, B. V. Hill, and R. G. Smits

December 9, 1952

Berkeley, California

Standard Distribution: Series E	Copy No.
Declassification Officer	1-6
Publication Officer	7
Patent Department	8-9
Information Division	10

UCRL-2046
Particle Accelerators and High-Voltage Machines

CAVITY DESIGN DATA FOR HIGH ENERGY LINEAR ACCELERATORS

S. W. Kitchen, A. D. Schelberg, B. V. Hill, and R. G. Smits

Radiation Laboratory, Department of Physics
University of California, Berkeley, California

December 9, 1952

ABSTRACT

Cavity design data necessary for the design of high energy resonant linear accelerators includes resonance, transit time factor, and shunt impedance information. This report presents such data in dimensionless form for several drift tube shapes as a function of an arbitrary parameter $d'\nu$ = constant, d' being drift tube bore diameter. The data is contained within the range of $\beta = 0.1$ to $\beta = 0.7$.

CAVITY DESIGN DATA FOR HIGH ENERGY LINEAR ACCELERATORS

S. W. Kitchen, A. D. Schelberg, B. V. Hill, and R. G. Smits

Radiation Laboratory, Department of Physics
University of California, Berkeley, California

December 9, 1952

INTRODUCTION

In order to study the possibilities of high energy resonant linear accelerators, it is necessary to have resonant, transit time factor, and shunt impedance data available up to and above the desired β. This report presents all the data of this nature collected in the course of seeking the best design of a specific accelerator. Consequently, the data is not complete in all respects. Nevertheless, the data nonessential to the present accelerator design may prove useful in further studies.

In a previous design data report on resonance,[1] the number of possible independent variables and the choice of variables was discussed in detail. In this report, the variables have been chosen to be the following: g/ℓ, β, D/d, D/d', $\checkmark$, d$\checkmark$, d'$\checkmark$, T, F and the shape of the drift tube. These symbols are defined in the Glossary. Resonant cavities have two other variables, the cavity shape and the mode of oscillation. For all of the data reported here, the cavity has the shape of a hollow circular cylinder and resonates in the TM_{01} mode. Other cavity shapes are possible, but they have not been examined.

RESONANCE

The drift tube shapes which were examined are shown in Figs. 1, 2, 3, and 4. The resonant data for these shapes were taken with the half cell cavities shown in Figs. 5, 6, and 7 using the apparatus shown in Fig. 8. All pertinent dimensions of the cavities and the drift tubes were measured to ± 0.001 inch and the resonant frequency was determined to at least 0.1 percent.

One feature of the cavity shown in Fig. 6 deserves special mention, the sliding rf joint between the piston and the cavity wall.* Previous ways of providing such a joint consisted of either spring fingers or a toroidal coil spring

---

* Patent applied for by A. E. C. for R. G. Smits.

in a slot, such as is used in the cavities of Figs. 5 and 6. Both methods have the objectionable feature of introducing a significant deviation from the desired geometry when the cavity length is short compared to its diameter. The inside-out pin vise construction of the new joint not only gives reliable rf contact, but also is only a minor deviation from the ideal geometry.

The first variable to be chosen arbitrarily was the drift tube shape. The second one was the product of the drift tube bore diameter and the frequency. If, as in the Berkeley 40-foot linear accelerator, the cavity diameter and the frequency had been chosen constant, the drift tube bore diameter would have become vanishingly small for high energies.

Figures 9, 10, 11, and 12 present dimensionless resonance data for the thick cylinder and pipe drift tubes for $d'\nu$ = 435.6 mc-in, and 290.4 mc-in respectively. Practical cavities designed from this data have resonated to within one percent and better of the design frequency. The reasons for error larger than 0.1 percent have been perturbations such as large pumping slots, drift tube stems, and/or tuning devices. For this reason, the effect of insertion of a standard gap splitter tuner or a drift tube stem whose diameter was half of d' was determined. In order of magnitude, at low β's (0.2), stems had a negligible effect, but at high β (0.5), the insertion of stems caused an increase in frequency of nearly one percent. On the other hand, the insertion of a gap splitter tuner decreased the frequency by nearly one percent at low β but had no visible effect at high β.

It will be observed that for a given D/d' and β in Figs. 10 and 12, $g/\mathcal{L}$ is smaller for the pipe configuration than for the thick cylinder drift tube. A similar relationship holds for Figs. 9 and 11, but is obscured by the use of different ordinate scales. Such behavior improved accelerator efficiency materially. A few data taken with the pipe configuration of d/d' = 1.3 indicated some improvement in this respect over that of d/d' = 1.5, but mechanical considerations led to a choice of 1.5 as the subject of further study.

Another possible way of achieving this effect, suggested by Prof. Chaim Richman, is to add a conical skirt to the thick cylinder design as shown in Fig. 3. This shape was studied at high β for optimum angle and length of the cone. Within the limited scope of the measurements, it was found that there was about 10 percent decrease in $g/\mathcal{L}$ over the thick cylinder without a skirt with $\theta = 45^{\circ}$ and c/2 = (2/3)(t/2). Pipe drift tubes on the other hand, give up to 30 percent decrease in $g/\mathcal{L}$ under similar conditions of D/d' and β.

On the basis of this data, the geometry of Fig. 4 was selected for further study. Figures 13, 14, 15, and 16 are the results. In each case, the stem diameter was half of d'. The gap splitter tuners were in the shape of thin cylindrical discs with a bore diameter equal to d'. One had an outer diameter equal to 2.78 d' with an assumed median thickness of 0.167 d'. The other had an outer diameter of 4.17 d' and an assumed thickness of 0.250 d'. The small differences due to the stems and tuners are only apparent in a detailed comparison. This drift tube shape, as expected, shows a significant decrease of g/ℓ over the straight pipe.

FIELD DISTRIBUTION

In addition to the factors previously mentioned, it is occasionally of interest to know the relative field distributions in a cell.[2] Figures 17, 18, 19, and 20 present such data for low and high β cells. The values of D/d' and β chosen for these examples are typical of those to be found in an optimum accelerator design. One fact that should be kept in mind is that the figures for the fields on the drift tube surfaces were taken with hemispheres. In order to compare this data to that taken in the same geometry with spheres, a correction factor must be applied. It might be expected that the factor would be two, since the volume is one-half of the sphere. The curvature of the surface, however, permits image effects to be significant. For the thick cylinder drift tube, the hemisphere correction in the H field to the observed $\delta\nu$ is 2.2 and in the E field is 2.0. For the pipes, the correction is 2.1 and 1.9 for the H and E fields respectively. These factors are a function of the surface curvature and therefore are presented primarily to illustrate the magnitude of the curvature correction rather than as constants of a drift tube shape. Further data of this nature is available in UCRL-2036.[3]

TRANSIT TIME FACTOR

The efforts toward determining the drift tube shape giving the smallest g/ℓ for given D/d' and β, were a result of the fact that better accelerating efficiency obtains for small g/ℓ. This accelerating efficiency is measured by the transit time factor or transit time coupling factor as it is frequently called. Often it is misleadingly abbreviated to just "transit time." The definition of this term is that T is equal to the ratio of the energy gained in crossing the gap to that which would have been gained in crossing the same gap having the same peak gap potential difference under d.c. conditions. For the general case, this definition may be written as:

$$T = \frac{\int_{-\ell/2}^{+\ell/2} E_o(x) \cos(\omega t + \phi)\, dx}{\int_{-\ell/2}^{+\ell/2} E_o(x)\, dx}$$

where ϕ is the rf phase at which the particle crosses the center of the gap, normally considered to be the stable phase angle of the accelerator. The exact evaluation of this equation can only be obtained from a differential analyzer, but an approximation good down to about $\beta = 0.15$ can be made on the assumption that $\Delta\beta/\beta$ is small for the gap in question. Then:

$$T = \frac{\int_{-\ell/2}^{\ell/2} E_o(x) \cos \frac{2\pi x}{\lambda} \cos \phi\, dx}{\int_{-\ell/2}^{\ell/2} E_o(x)\, dx}$$

The data presented in Figs. 21, 22, 23, and 24 were calculated from data taken in the 20-inch cavity of Fig. 7 by the perturbation technique. This technique, together with the associated apparatus and procedures used, has been fully described in a recent report.[2] The precision of the data is on the order of 0.2 percent, but the accuracy is determined by the validity of the assumptions of $\Delta\beta/\beta$ being small. A quantitative idea of the gain in T of pipes over thick cylinders for the same D/d' and β can be obtained by comparing Figs. 17 and 18. The net gain in T is but 10 percent as compared to ~30 percent improvement in g/ℓ. The reduced gain results from the fact that for the same g/ℓ and β, the thick cylinders have better T values. When combined with the gain in shunt impedance, however, the total advantage in power requirements for the pipes over the thick cylinders for $\beta = 0.5$ is about 30 percent.

SHUNT IMPEDANCE

The theoretical shunt impedance (shunt resistance) of a cell in an accelerator can also be obtained from perturbation measurements[2] on a single cell. In terms of the observed frequency shift, such as in Figs. 17 through 20, the shunt resistance is:

$$Z_s = \frac{\frac{\mu_o}{\varepsilon_o}\,\sigma\,\Delta\left[\oint (\delta\nu)^{1/2}\,ds\right]^2}{2\int\left[\xi\,(\delta\nu)_D - (\delta\nu)_M\right] dA}$$

where σ is conductivity, Δ is skin depth, $\delta\nu$ is frequency shift, ξ is a constant of the measuring system, $\oint \dot{M}\,ds$ is the line integral enclosing maximum flux, $\frac{\mu_o}{\varepsilon_o}$ is the impedance squared of the cavity dielectric, and the $\int G\,dA$ is the surface integral of the $\delta\nu$ due to the magnetic field.

This formula is not in convenent form for scaling. Consequently, a dimensionless figure of merit for shunt impedance, called F factor, was obtained by calculating the ratio of the shunt impedance per unit length of the cell under consideration from the above formula to the shunt impedance per unit length of an unloaded cylindrical cavity resonating at the same frequency in the same mode. Since the shunt impedance of a cell incorporated in an accelerator (i.e., without end walls) is the value of interest, the values of F in Tables I and II and in Fig. 25 were computed on this basis. An approximation to the shunt impedance of a cell with end walls, may be obtained by dividing $Z_s(\lambda)$ by $1 + \frac{a}{\ell}$ where a is the radius $a(\lambda)$ and the length $\ell = \beta\lambda$.

The data in Tables I and II are presented for the purpose of indicating the relative magnitudes of the integrals in Z_s, particularly the two portions of the surface integral in the denominator. For example, the relative value of this integral over the cavity wall and that of this integral over the drift tube surface is a measure of the relative rf losses on the two surfaces. In using these tables, it should be kept in mind that the values of F given are those calculated from the data. As can be seen in Fig. 25, there is appreciable scattering of these points about the family of curves believed to be the best estimates of the true values. Although these were the data obtained by the technique described in UCRL-1947, in general only one measurement with this technique was made at each data point. The best estimates under the circumstances of the limits of error are ± 0.04 for the thick cylinder drift tubes and ± 0.02 for the pipes.

Although no shunt impedance data were taken on the bulbous pipe configuration, an estimate of the lower limit can be made by analogy to the shunt resistance relationship between the thick cylinder drift tube with and without the conical skirt. For the optimum skirted shape previously described at $\beta \sim 0.5$, the shunt resistance was 7 percent higher than the thick cylinder drift having the same g/ℓ and β, but was about 5 percent lower than the one having the same D/d' and β. Since g/ℓ and β are usually the independent variables in accelerator design, as a rule of thumb one can say that the shunt impedance of an accelerator with bulbous pipes will be slightly better than the same design with straight pipes.

ACKNOWLEDGEMENTS

The authors are principally responsible for the data contained in this report. Significant contributions, however, are gratefully acknowledged from D. B. Cummings, S. P. Stone, A. J. Schwemin, and S. A. Colgate. Our gratitude is also expressed to Professors L. W. Alvarez, A. Longacre, and W. K. H. Panofsky for advice and encouragement.

Information Division
12-16-52 bw

REFERENCES

1. S. W. Kitchen and R. G. Smits, University of California Radiation Laboratory Report No. UCRL-1739
2. S. W. Kitchen and A. D. Schelberg, University of California Radiation Laboratory Report No. UCRL-1947
3. A. D. Schelberg, University of California Radiation Laboratory Report No. UCRL-2036

GLOSSARY

D	Cavity inside diameter
d	Outer diameter of the drift tube
d'	Bore diameter of the drift tube
g	Geometric gap length
ℓ	Repeat or cell length
β	ℓ/λ and v/c of an in-phase particle
λ	Free space wavelength at cavity frequency
ν	Cavity frequency
$\delta\nu$	Change in cavity frequency due to perturbing sphere
T	Transit time coupling factor
Z_s	Shunt resistance
Z_s/ℓ	Average shunt resistance per unit length of a cell
F	Ratio of Z_s/ℓ to the shunt resistance per unit length of an unloaded cavity resonating at the same frequency

$$\oint M ds = \oint (\delta\nu)^{1/2} ds$$

$$\int G da = \int \left[\xi (\delta\nu)_d - (\delta\nu)_M \right] dA$$

TABLE I

Thick Cylinder Drift Tube Shunt Impedance Data*

D/d'	β	$\left[\int E d\ell\right]^2$	$\int H^2 dS$ over drift tube	$\int H^2 dS$ over cavity	F
17.0	0.15	42.62 kc-in^2	63.04 kc-in^2	124.6 kc-in^2	0.98
	0.25	73.30	67.08	125.6	0.99
16.0	0.30	82.3	105.8	108.3	0.83
	0.35	96.2	107.2	107.6	0.83
	0.40	108.2	108.5	105.9	0.82
	0.50	129.3	126.1	101.7	0.74
15.3	0.40	94.9	128.0	95.4	0.69
	0.50	114.7	138.3	89.8	0.65
14.6	0.50	102.2	137.3	82.3	0.61
	0.60	122.5	173.5	70.1	0.54

*Scaled for d'ν = 435.6 mc-in

TABLE II

Pipe Drift Tube Shunt Impedance Data*

D/d'	β	$\left[\int E d\ell\right]^2$	$\int H^2 dS$ over drift tube	$\int H^2 dS$ over cavity	F
15.3	0.350	105.8 kc-in^2	146.2 kc-in^2	93.3 kc-in^2	0.82
	0.400	120.5	157.4	92.3	0.78
	0.500	142.9	166.7	84.9	0.72
	0.600	166.7	179.9	76.5	0.70
16.0	0.350	116.1	145.6	105.3	0.86
	0.400	131.0	159.3	102.7	0.81
	0.500	159.3	177.8	97.2	0.75
16.6	0.350	122.3	137.4	115.2	0.90
	0.400	138.2	146.6	113.3	0.86
	0.500	169.0	177.7	108.1	0.77
	0.600	196.1	192.6	101.8	0.72
	0.700	216.3	206.1	94.3	0.67
17.0	0.300	109.2	119.8	126.6	0.96
	0.350	128.6	117.2	125.8	0.98
	0.400	144.4	143.9	125.7	0.87
	0.500	177.0	154.8	121.2	0.85
	0.600	215.3	190.1	114.1	0.76

* Scaled for d'ν = 435.6 mc-in

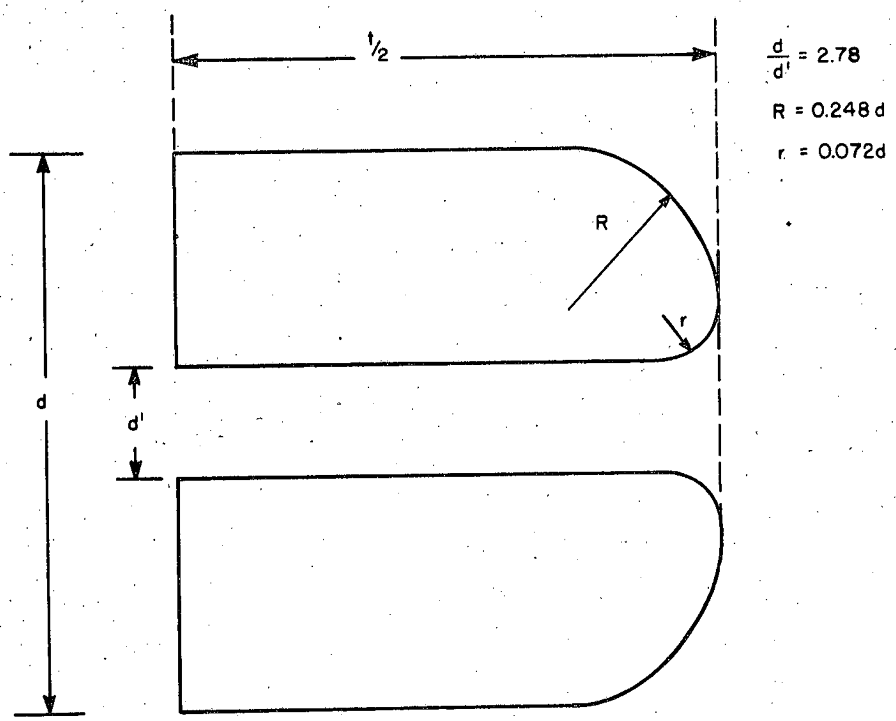

THICK CYLINDER DRIFT TUBE CONFIGURATION

MU-5049

Fig. 1

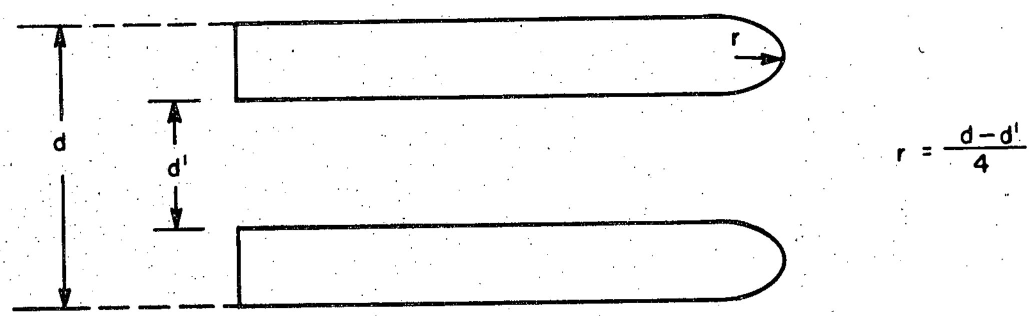

PIPE DRIFT TUBE CONFIGURATION

FIG. 2

MU-5050

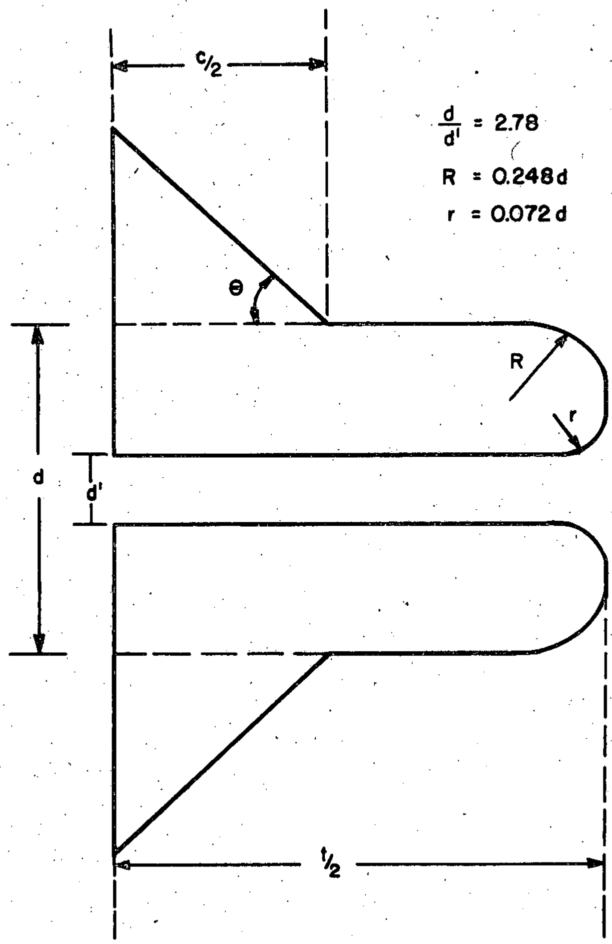

THICK CYLINDER DRIFT TUBE WITH CONICAL SKIRT

MU-5051

Fig. 3

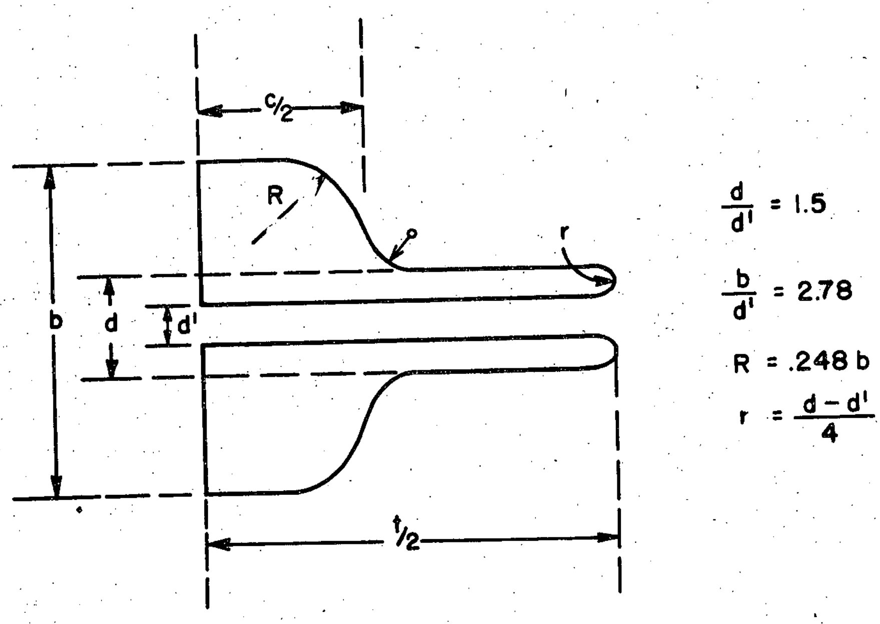

BULBOUS PIPE DRIFT TUBE CONFIGURATION

MU-5052

Fig. 4

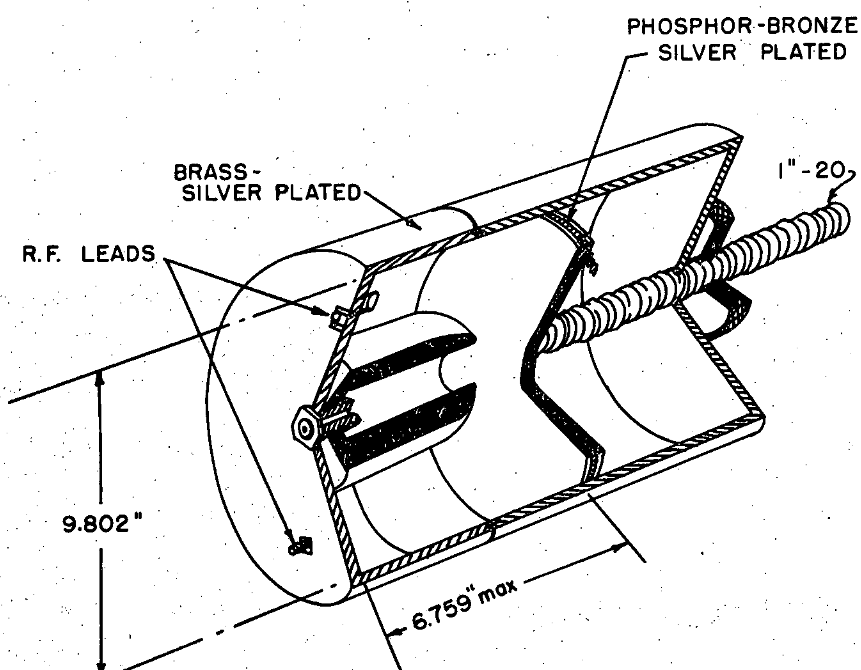

9.8" PRECISION CAVITY MU3418

Fig. 5

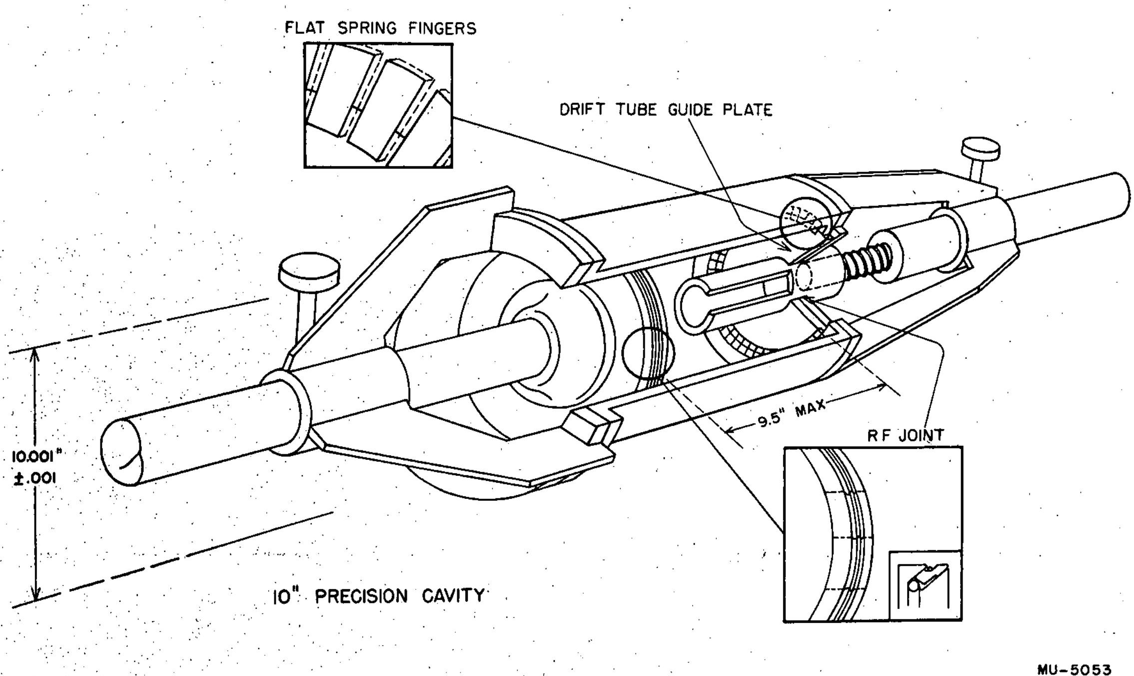
FLAT SPRING FINGERS
DRIFT TUBE GUIDE PLATE
10.001"
±.001
9.5" MAX
RF JOINT
10" PRECISION CAVITY
MU-5053

Fig. 6

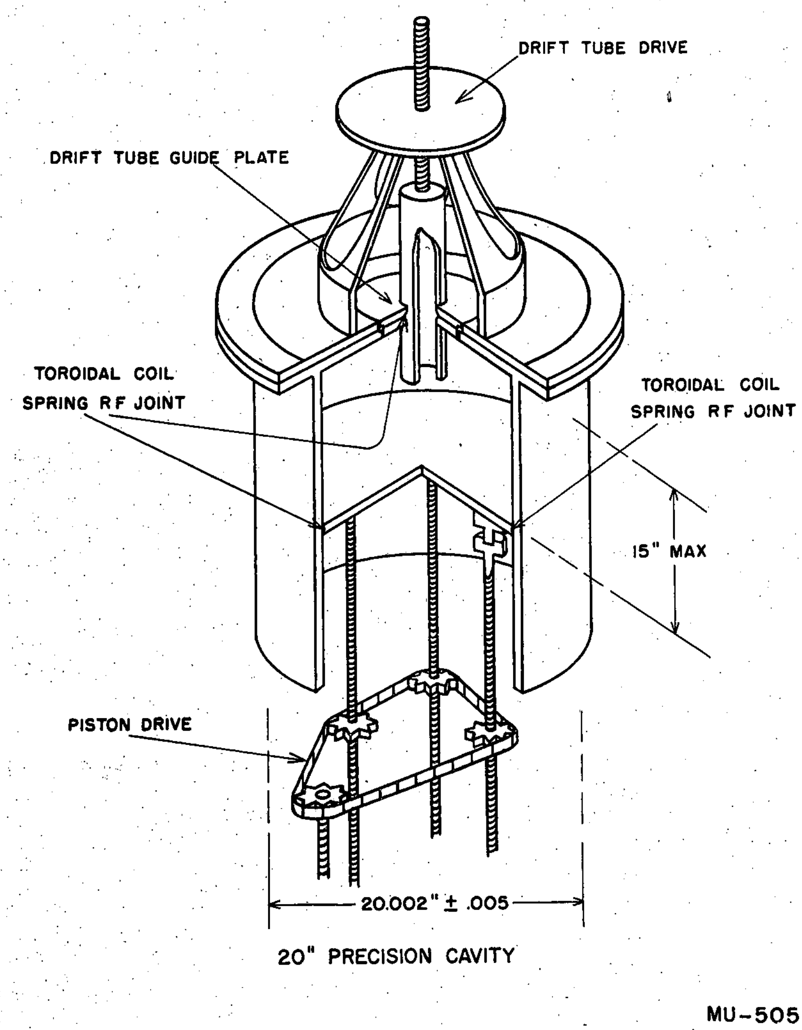
DRIFT TUBE DRIVE
DRIFT TUBE GUIDE PLATE
TOROIDAL COIL
SPRING RF JOINT
TOROIDAL COIL
SPRING RF JOINT
15" MAX
PISTON DRIVE
20.002" ± .005
20" PRECISION CAVITY
MU-5054

Fig. 7a

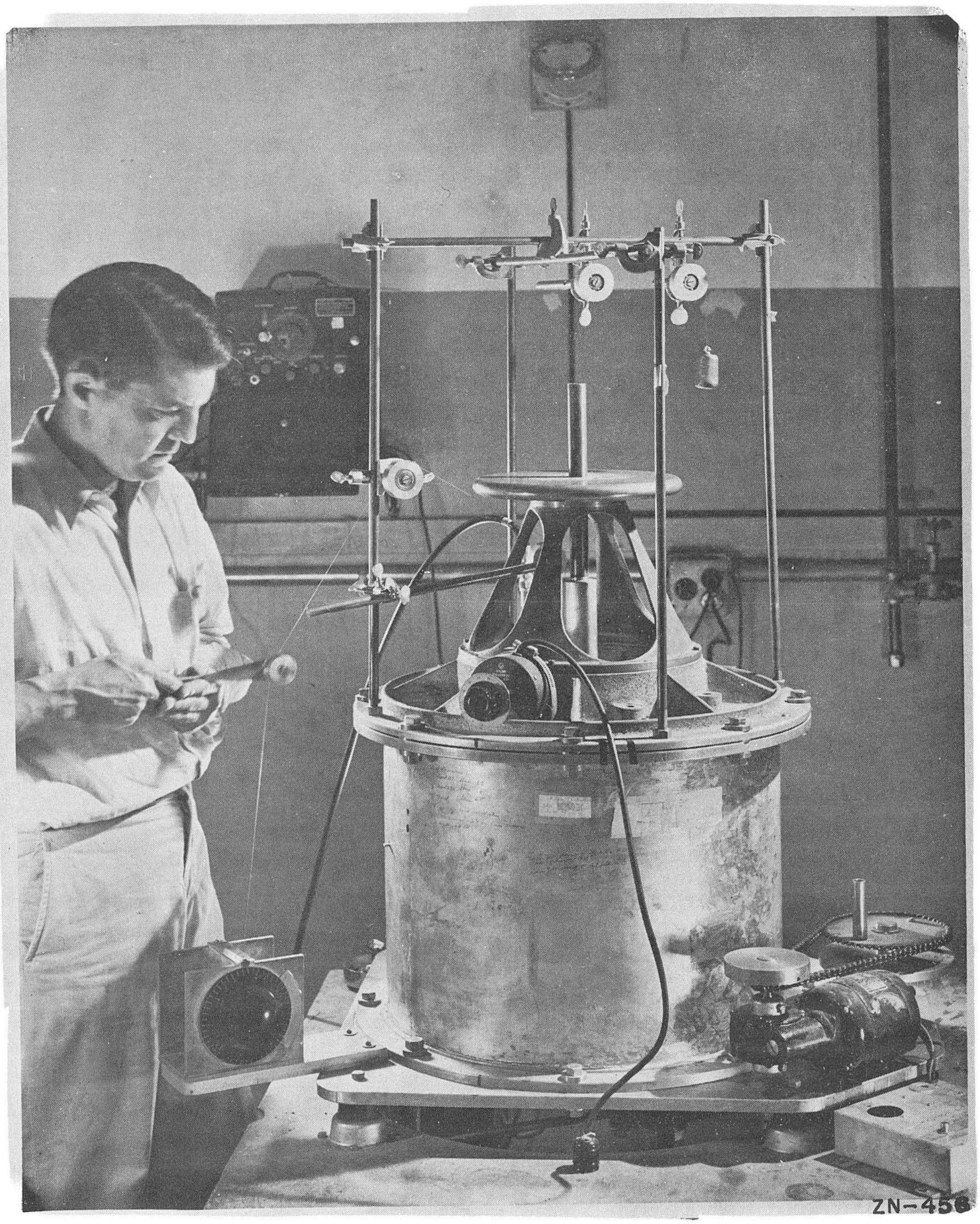

Fig. 7b

20 in. cavity apparatus for field measurements

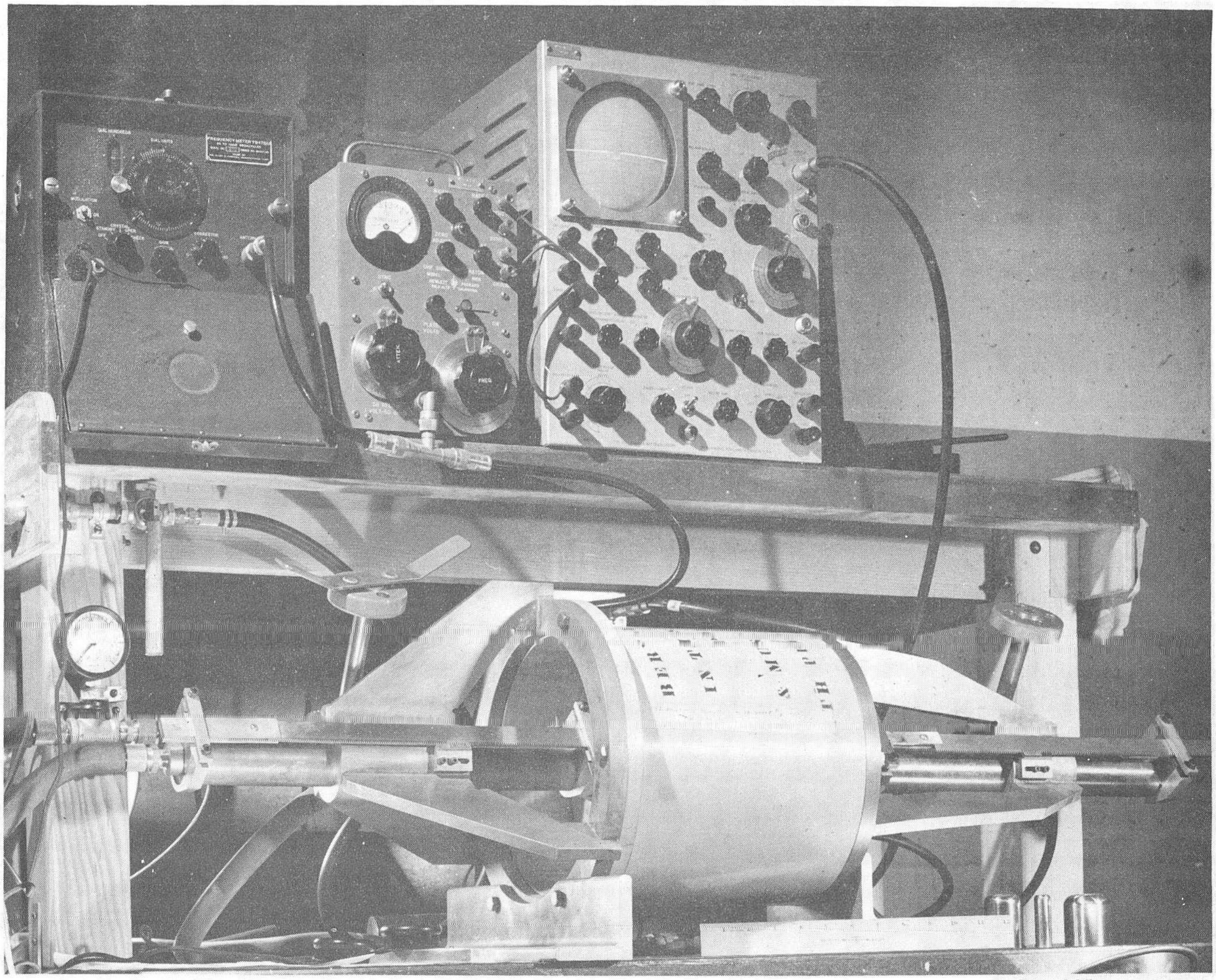

ZN-485

Fig. 8

10 in. cavity apparatus for field measurements

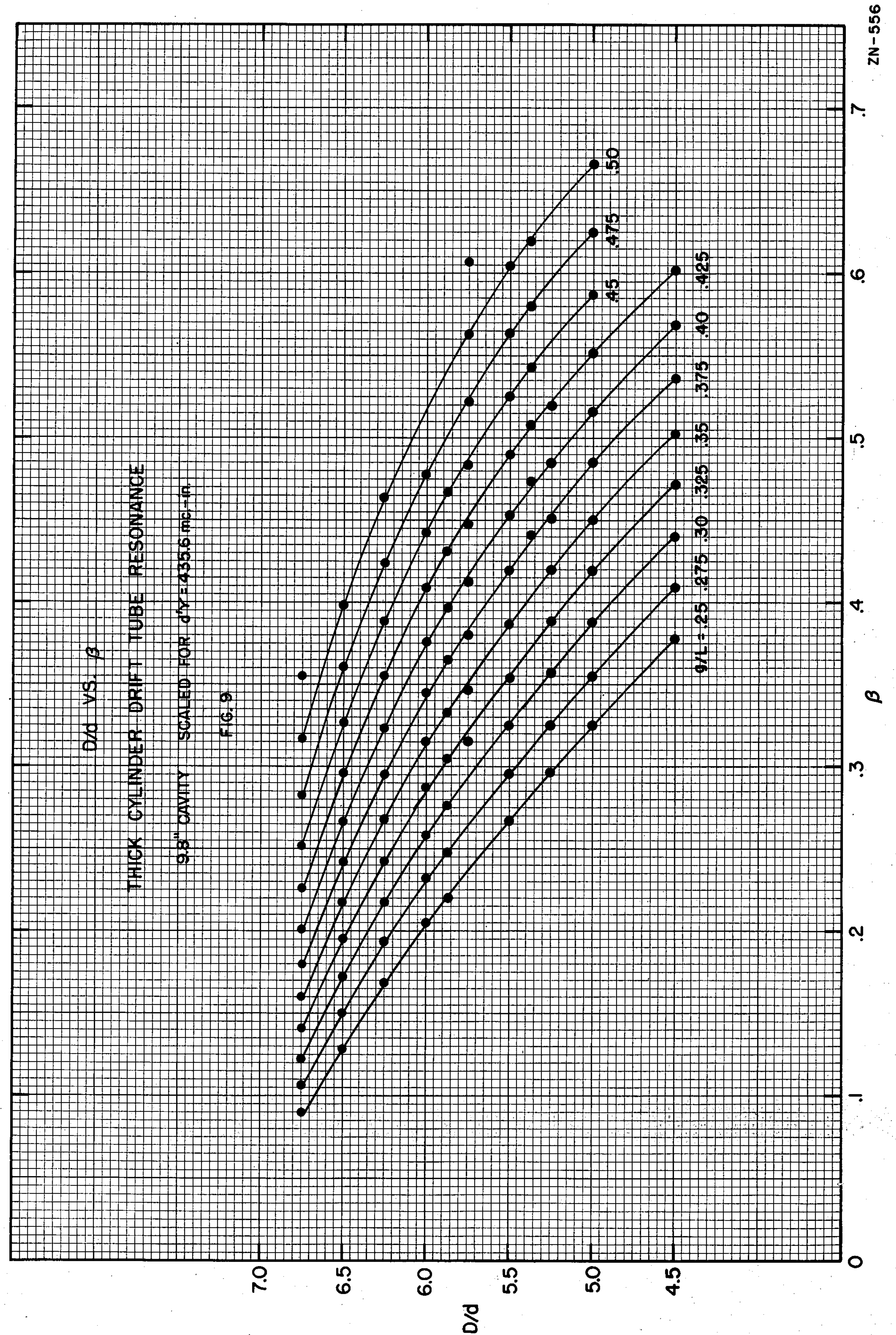
ZN-556
D/d VS. β
THICK CYLINDER DRIFT TUBE RESONANCE
9.8" CAVITY SCALED FOR d'Y = 435.6 mc.-in.
FIG. 9
g/L = .25 .275 .30 .325 .35 .375 .40 .425 .45 .475 .50
β
0 .1 .2 .3 .4 .5 .6 .7
D/d
7.0 6.5 6.0 5.5 5.0 4.5

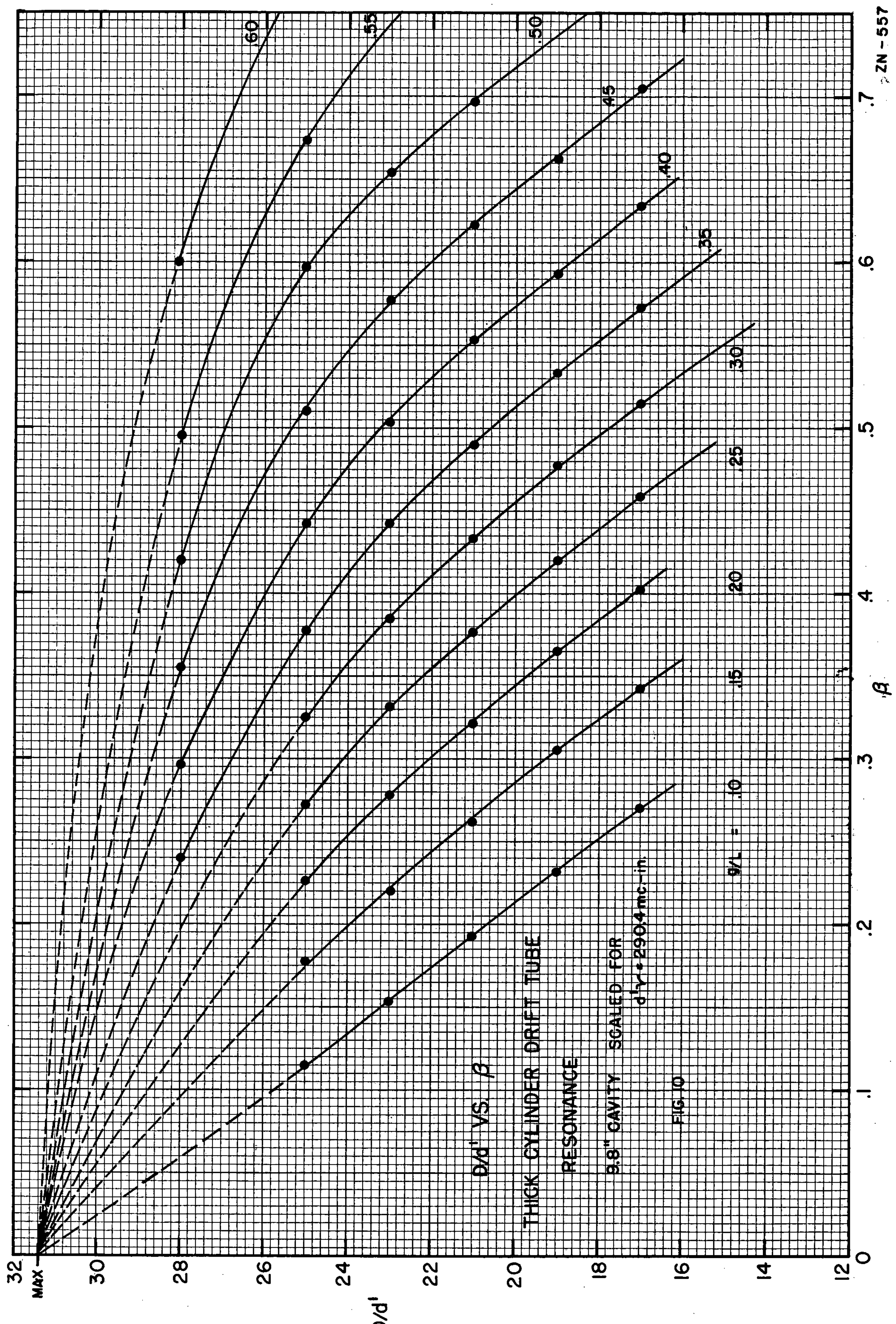
D/d' VS. β
THICK CYLINDER DRIFT TUBE
RESONANCE
9.8" CAVITY SCALED FOR
d'ν = 290.4 mc.-in.
FIG. 10
g/L = .10
.15
.20
.25
.30
.35
.40
.45
.50
.55
.60
β
D/d'
MAX
32
30
28
26
24
22
20
18
16
14
12
0
.1
.2
.3
.4
.5
.6
.7
ZN-557

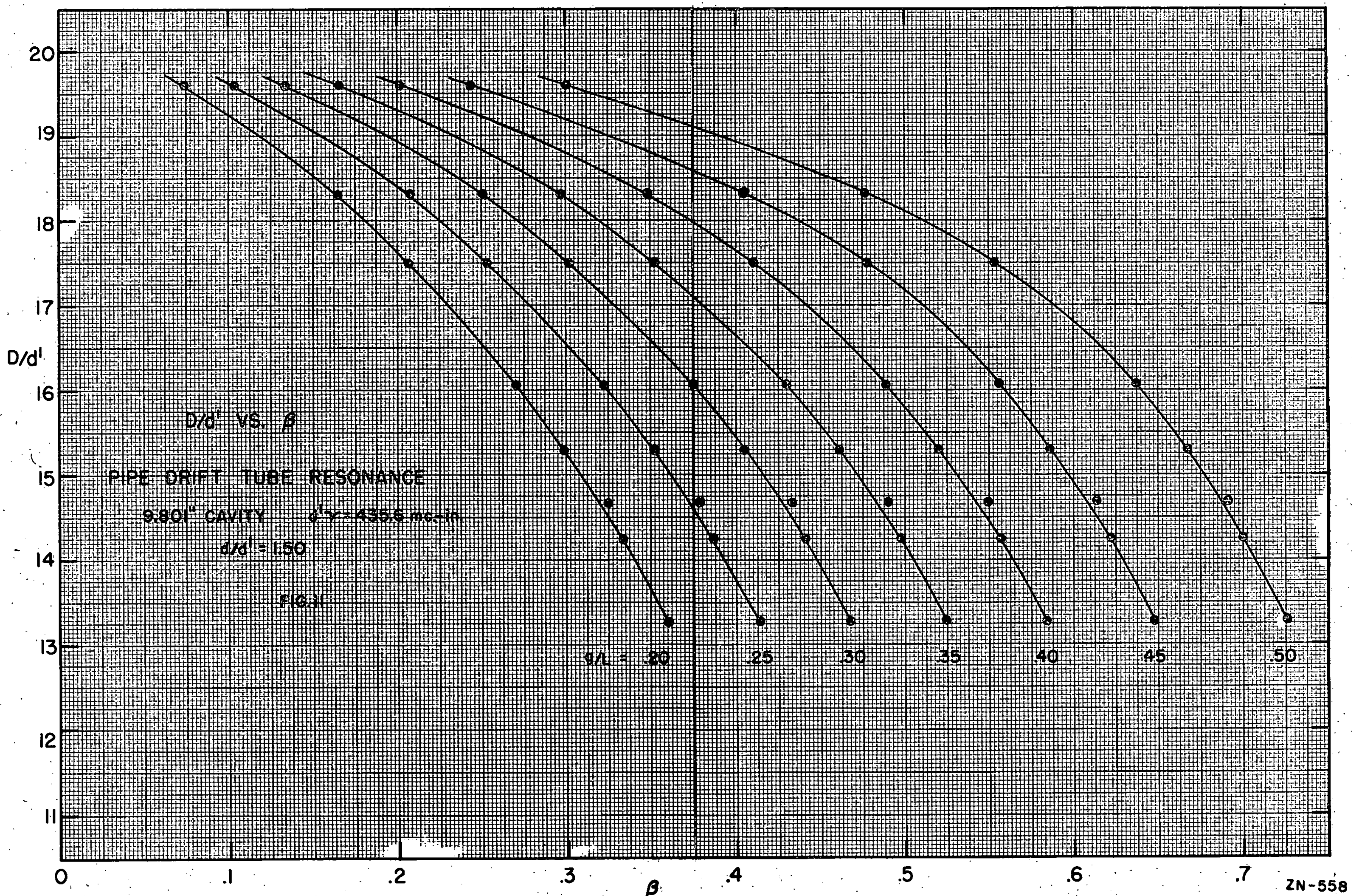
D/d' VS. β
PIPE DRIFT TUBE RESONANCE
9.801" CAVITY d'ν = 435.6 mc-in
d/d' = 1.50
FIG. 11
g/L = .20
.25
.30
.35
.40
.45
.50
D/d'
β
20
19
18
17
16
15
14
13
12
11
0
.1
.2
.3
.4
.5
.6
.7
ZN-558

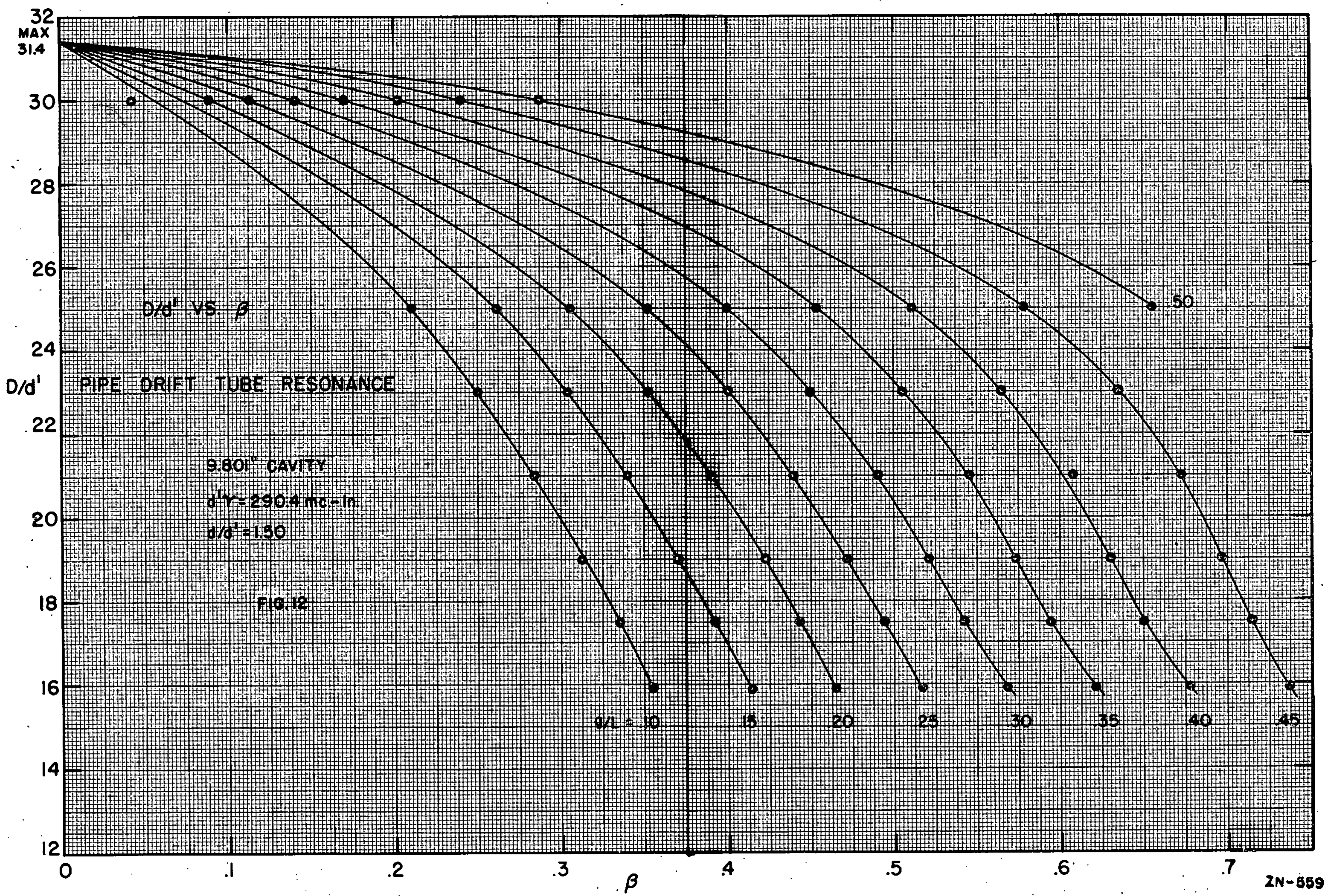
D/d' VS. β
PIPE DRIFT TUBE RESONANCE
9.801" CAVITY
d'γ = 290.4 mc-in
d/d' = 1.50
FIG. 12
D/d'
β
32
MAX 31.4
30
28
26
24
22
20
18
16
14
12
0
.1
.2
.3
.4
.5
.6
.7
g/L = .10
.15
.20
.25
.30
.35
.40
.45
.50
ZN-559

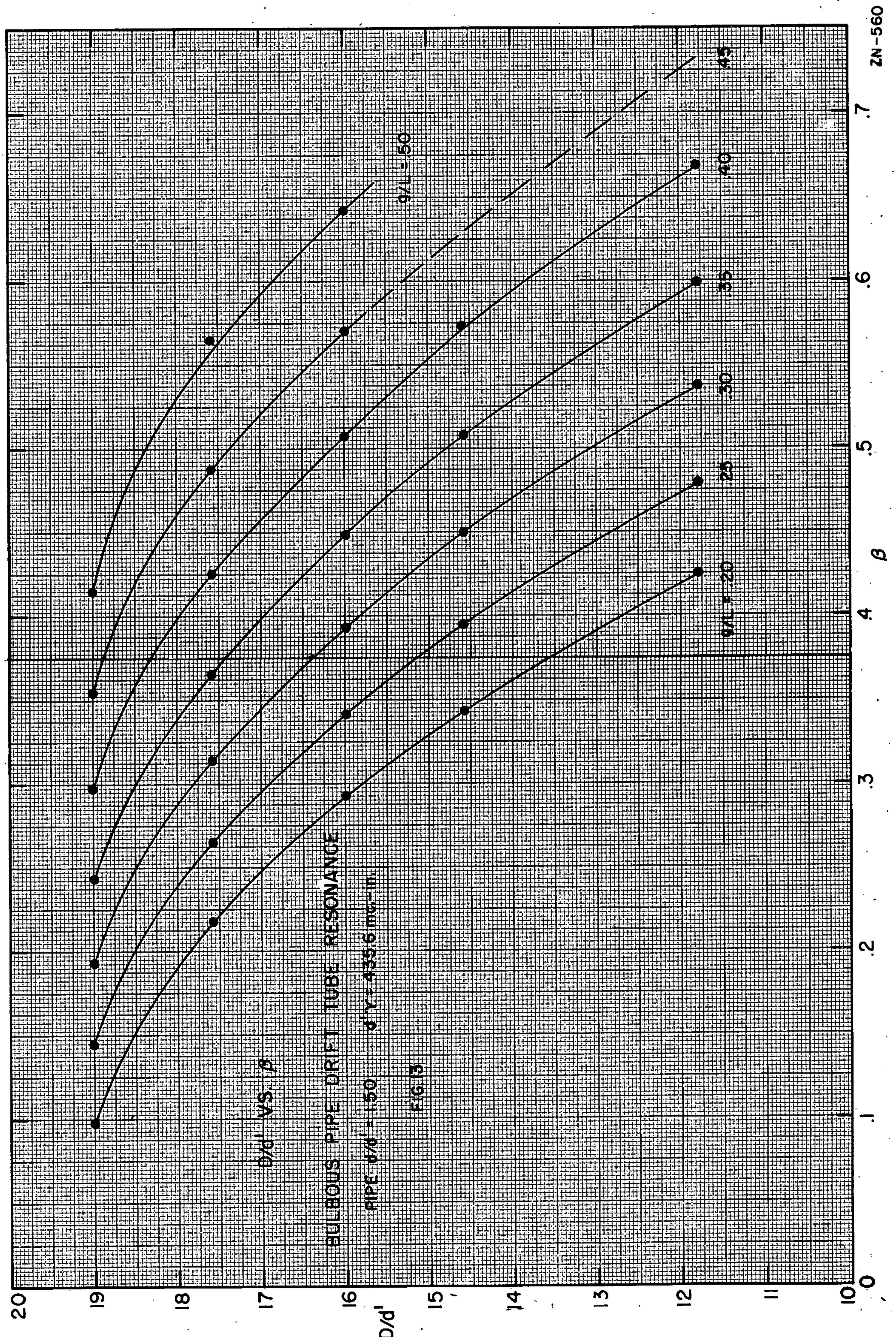
D/d' VS. β
BULBOUS PIPE DRIFT TUBE RESONANCE
PIPE d/δ' = 1.50
d'γ = 435.6 mc.-in.
g/L = .20
.25
.30
.35
.40
.45
g/L = .50
β
D/d'
0
.1
.2
.3
.4
.5
.6
.7
10
11
12
13
14
15
16
17
18
19
20
ZN-560

FIG 3

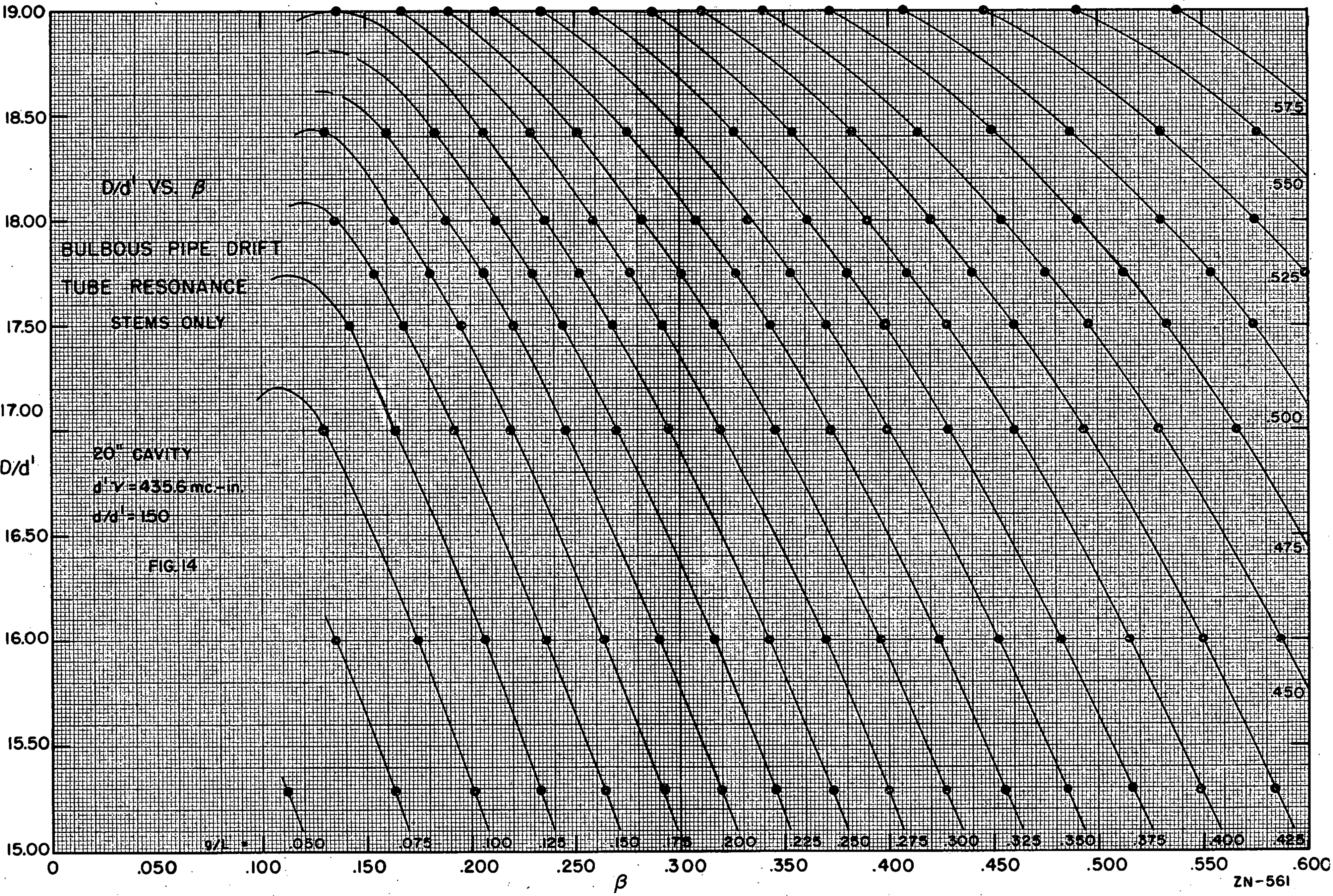
D/d' VS. β
BULBOUS PIPE DRIFT
TUBE RESONANCE
STEMS ONLY
20" CAVITY
d'ν = 435.6 mc-in.
d/d' = 1.50
D/d'
β
g/L = .050 .075 .100 .125 .150 .175 .200 .225 .250 .275 .300 .325 .350 .375 .400 .425 .450 .475 .500 .525 .550 .575
15.00 15.50 16.00 16.50 17.00 17.50 18.00 18.50 19.00
0 .050 .100 .150 .200 .250 .300 .350 .400 .450 .500 .550 .600
ZN-561

FIG. 14

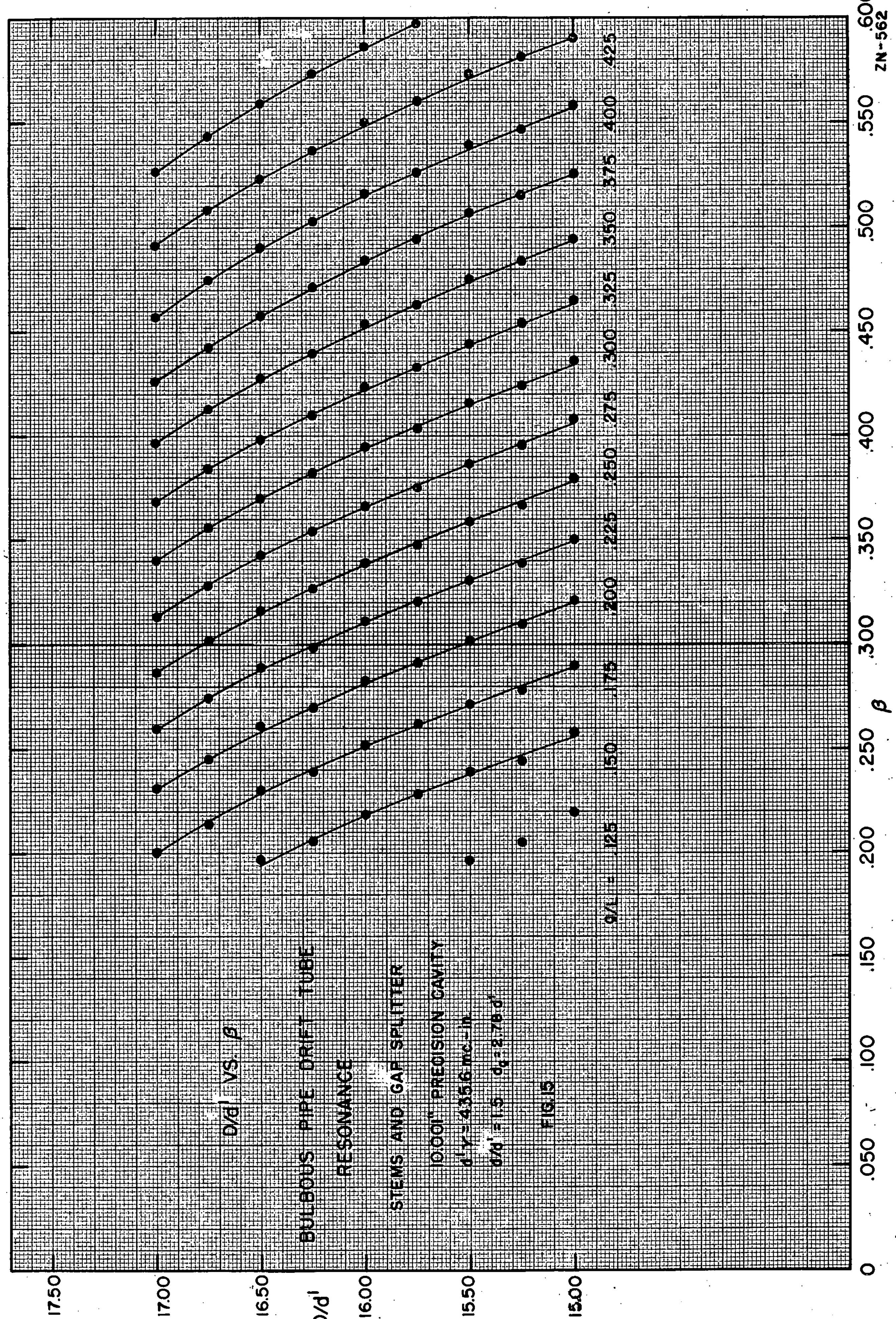
D/d' VS. β
BULBOUS PIPE DRIFT TUBE
RESONANCE
STEMS AND GAP SPLITTER
.0001" PRECISION CAVITY
d' γ = 435.6 mc.-in.
d/d' = 1.5 d_c = 2.78 d'
g/L = .125 .150 .175 .200 .225 .250 .275 .300 .325 .350 .375 .400 .425
D/d'
17.50
17.00
16.50
16.00
15.50
15.00
β
0 .050 .100 .150 .200 .250 .300 .350 .400 .450 .500 .550 .600
ZN-562

FIG. 15

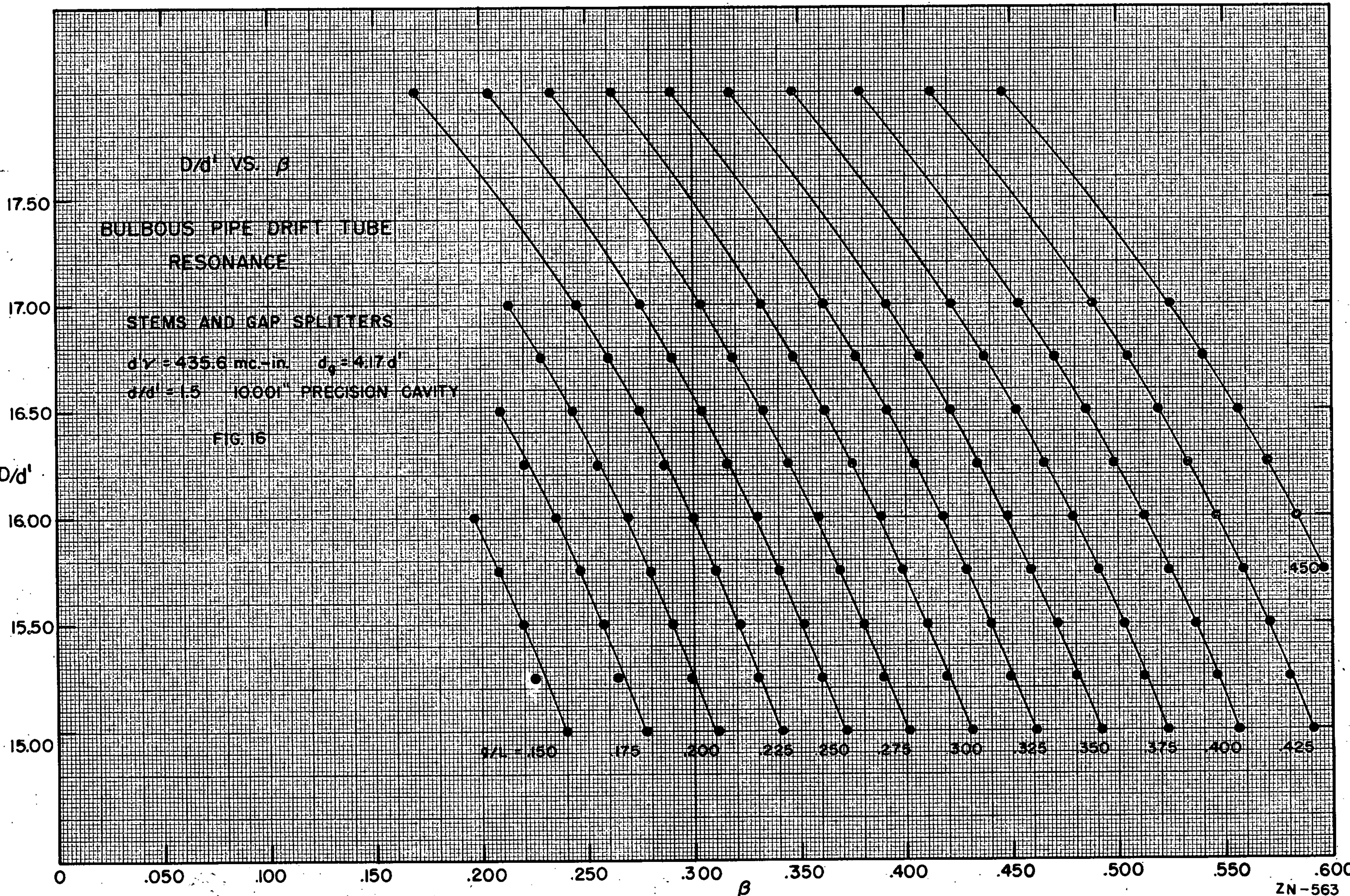
D/d' VS. β
BULBOUS PIPE DRIFT TUBE
RESONANCE
STEMS AND GAP SPLITTERS
d'ν = 435.6 mc.-in. d_g = 4.17 d'
d/d' = 1.5 10.001" PRECISION CAVITY
FIG. 16
17.50
17.00
16.50
D/d'
16.00
15.50
15.00
g/L = .150
.175
.200
.225
.250
.275
.300
.325
.350
.375
.400
.425
.450
0
.050
.100
.150
.200
.250
.300
.350
.400
.450
.500
.550
.600
β
ZN-563

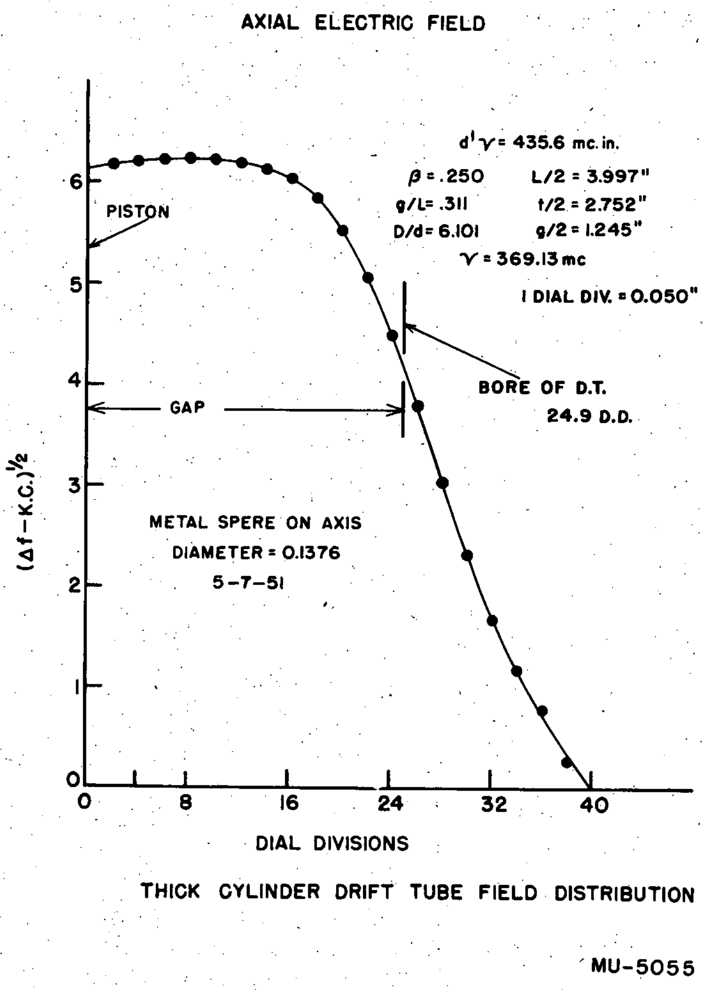
AXIAL ELECTRIC FIELD
d'γ = 435.6 mc.in.
β = .250
L/2 = 3.997"
g/L = .311
t/2 = 2.752"
D/d = 6.101
g/2 = 1.245"
γ = 369.13 mc
1 DIAL DIV. = 0.050"
PISTON
GAP
BORE OF D.T.
24.9 D.D.
METAL SPERE ON AXIS
DIAMETER = 0.1376
5-7-51
(Δf - K.C.)^½
0
1
2
3
4
5
6
0
8
16
24
32
40
DIAL DIVISIONS
THICK CYLINDER DRIFT TUBE FIELD DISTRIBUTION
MU-5055

Fig. 17a

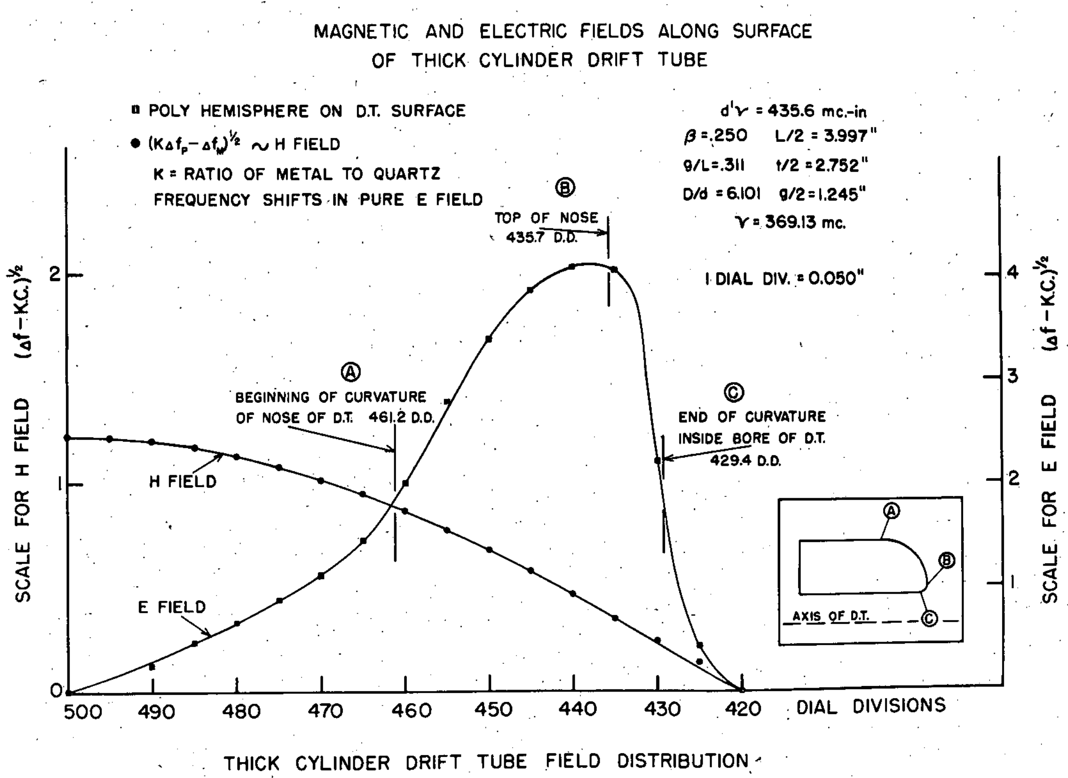

MU-5056

Fig. 17b

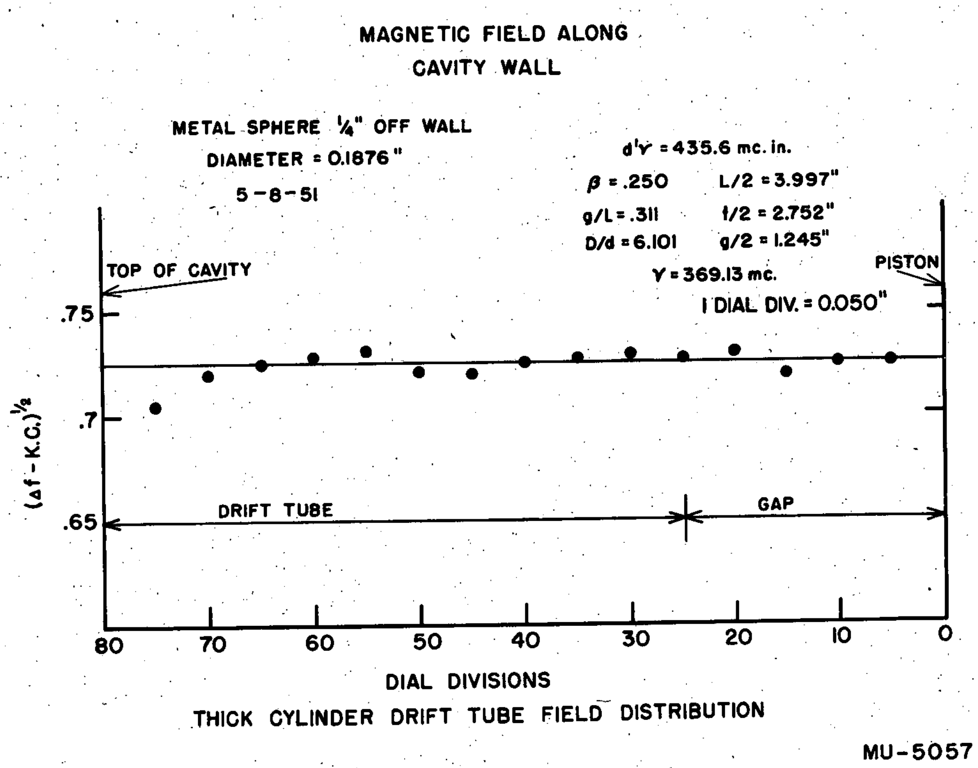
MAGNETIC FIELD ALONG
CAVITY WALL
METAL SPHERE ¼" OFF WALL
DIAMETER = 0.1876"
5-8-51
d'γ = 435.6 mc. in.
β = .250
L/2 = 3.997"
g/L = .311
ℓ/2 = 2.752"
D/d = 6.101
g/2 = 1.245"
γ = 369.13 mc.
1 DIAL DIV. = 0.050"
TOP OF CAVITY
PISTON
.75
.7
.65
(Δf - K.C.)^½
DRIFT TUBE
GAP
80
70
60
50
40
30
20
10
0
DIAL DIVISIONS
THICK CYLINDER DRIFT TUBE FIELD DISTRIBUTION
MU-5057

Fig. 17c

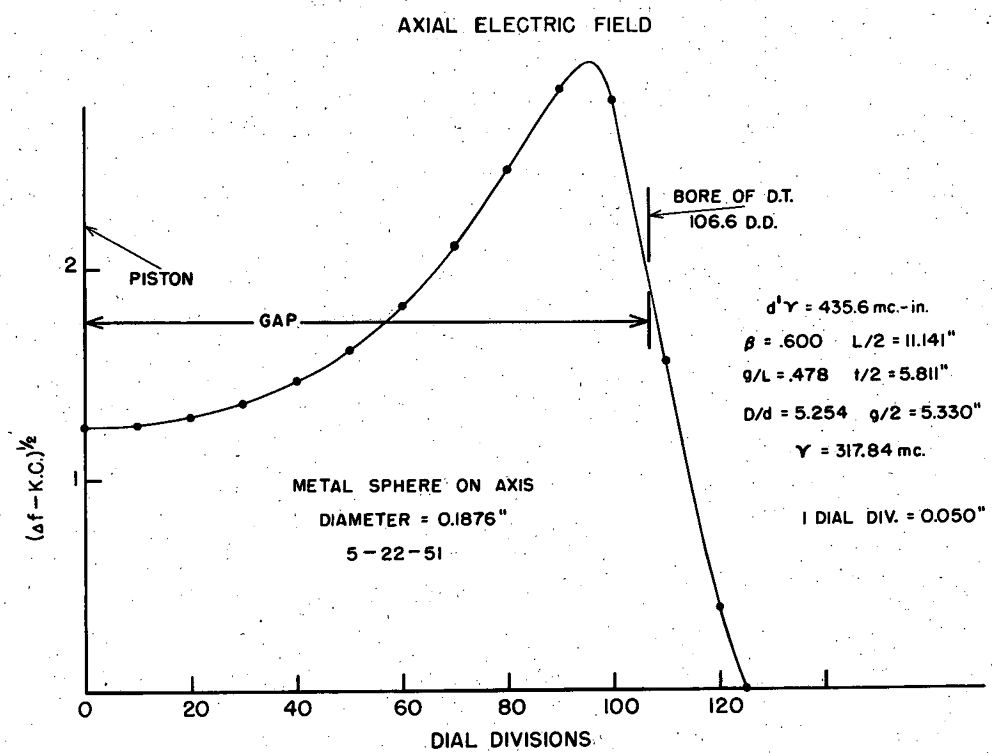

THICK CYLINDER DRIFT TUBE FIELD DISTRIBUTION

MU-5058

Fig. 18a

MAGNETIC AND ELECTRIC FIELDS ALONG SURFACE
OF THICK CYLINDER DRIFT TUBE

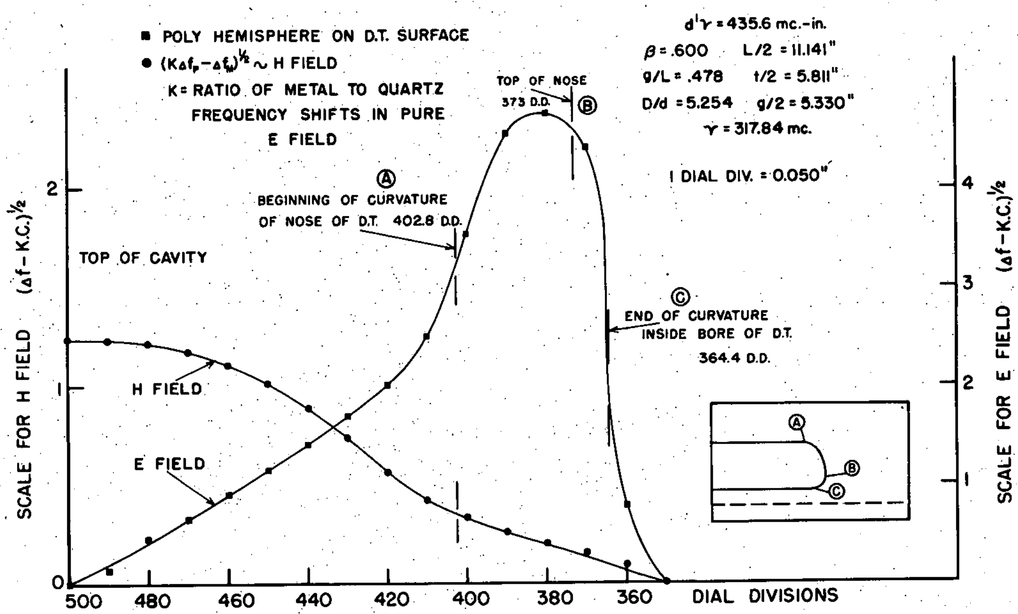

THICK CYLINDER DRIFT TUBE FIELD DISTRIBUTION

FIG. 18b

MU-5059

MAGNETIC FIELD ALONG CAVITY WALL

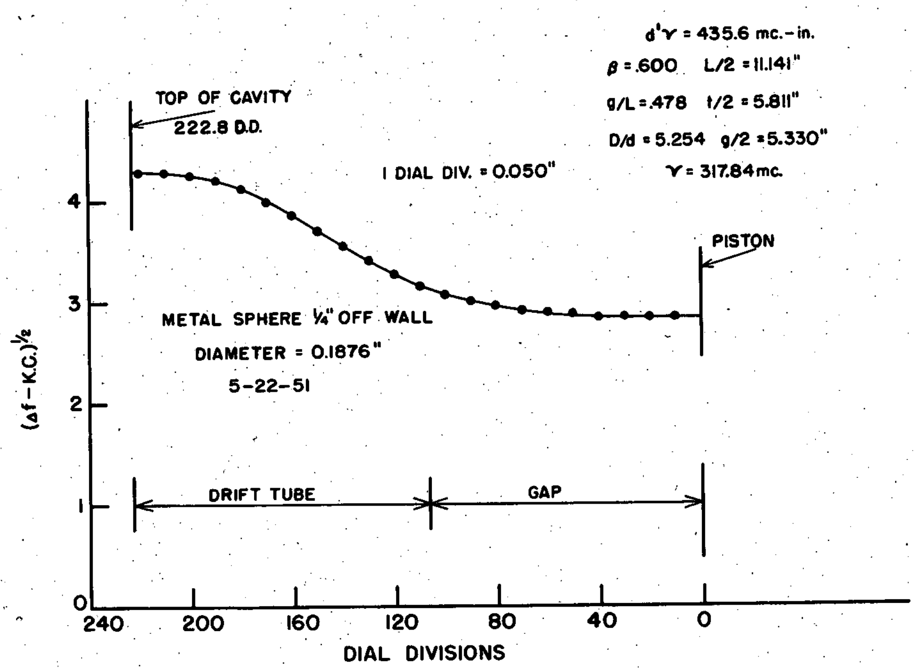

THICK CYLINDER DRIFT TUBE FIELD DISTRIBUTION

FIG. 18c

MU-5060

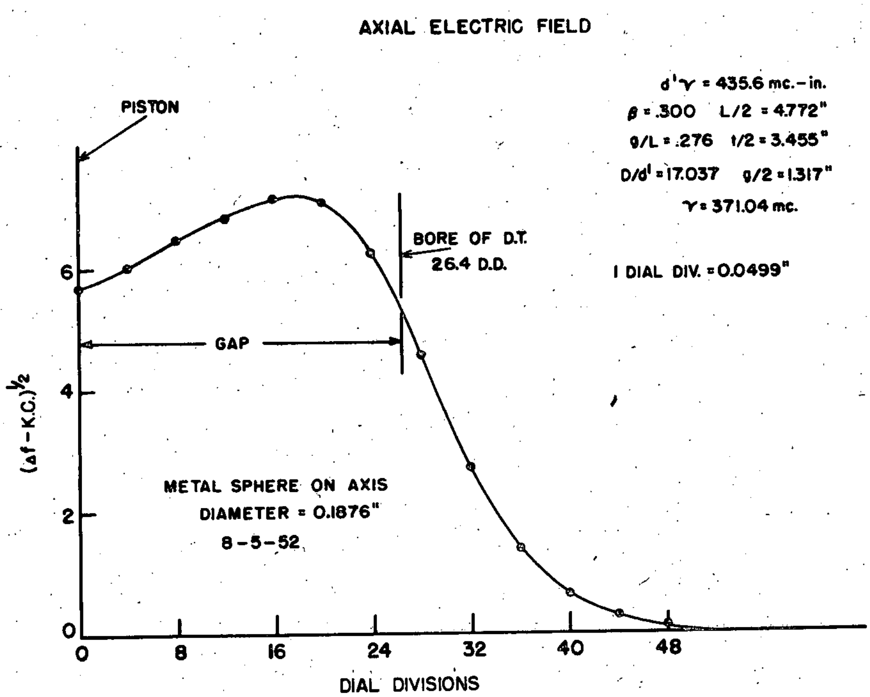

PIPE DRIFT TUBE FIELD DISTRIBUTION

FIG.19a

MU-5061

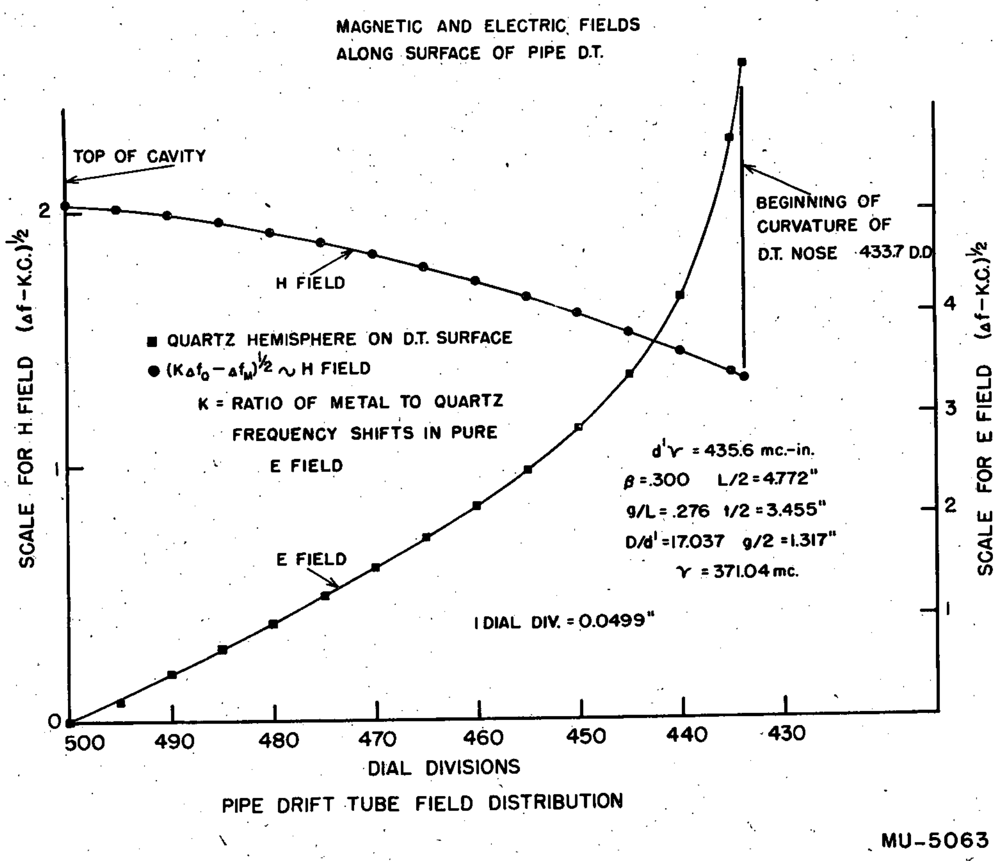
MAGNETIC AND ELECTRIC FIELDS
ALONG SURFACE OF PIPE D.T.
TOP OF CAVITY
BEGINNING OF
CURVATURE OF
D.T. NOSE 433.7 D.D.
H FIELD
■ QUARTZ HEMISPHERE ON D.T. SURFACE
● (KΔf₀ − Δf_M)^½ ∼ H FIELD
K = RATIO OF METAL TO QUARTZ
FREQUENCY SHIFTS IN PURE
E FIELD
d′λ = 435.6 mc.-in.
β = .300 L/2 = 4.772"
g/L = .276 t/2 = 3.455"
D/d′ = 17.037 g/2 = 1.317"
λ = 371.04 mc.
E FIELD
1 DIAL DIV. = 0.0499"
SCALE FOR H FIELD (Δf − K.C.)^½
SCALE FOR E FIELD (Δf − K.C.)^½
0
1
2
3
4
500
490
480
470
460
450
440
430
DIAL DIVISIONS
PIPE DRIFT TUBE FIELD DISTRIBUTION
MU-5063

Fig. 19b

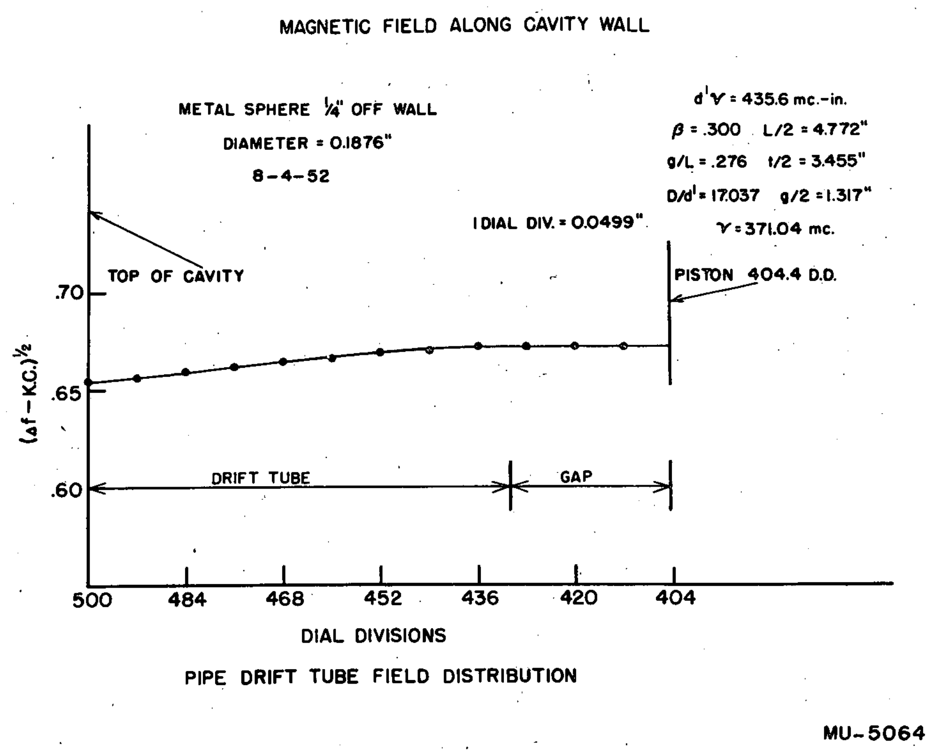
MAGNETIC FIELD ALONG CAVITY WALL
METAL SPHERE 1/4" OFF WALL
DIAMETER = 0.1876"
8-4-52
d'γ = 435.6 mc.-in.
β = .300 L/2 = 4.772"
g/L = .276 t/2 = 3.455"
D/d' = 17.037 g/2 = 1.317"
γ = 371.04 mc.
1 DIAL DIV. = 0.0499"
TOP OF CAVITY
PISTON 404.4 D.D.
.70
.65
.60
(Δf - K.C.)^½
DRIFT TUBE
GAP
500
484
468
452
436
420
404
DIAL DIVISIONS
PIPE DRIFT TUBE FIELD DISTRIBUTION
MU-5064

Fig. 19c

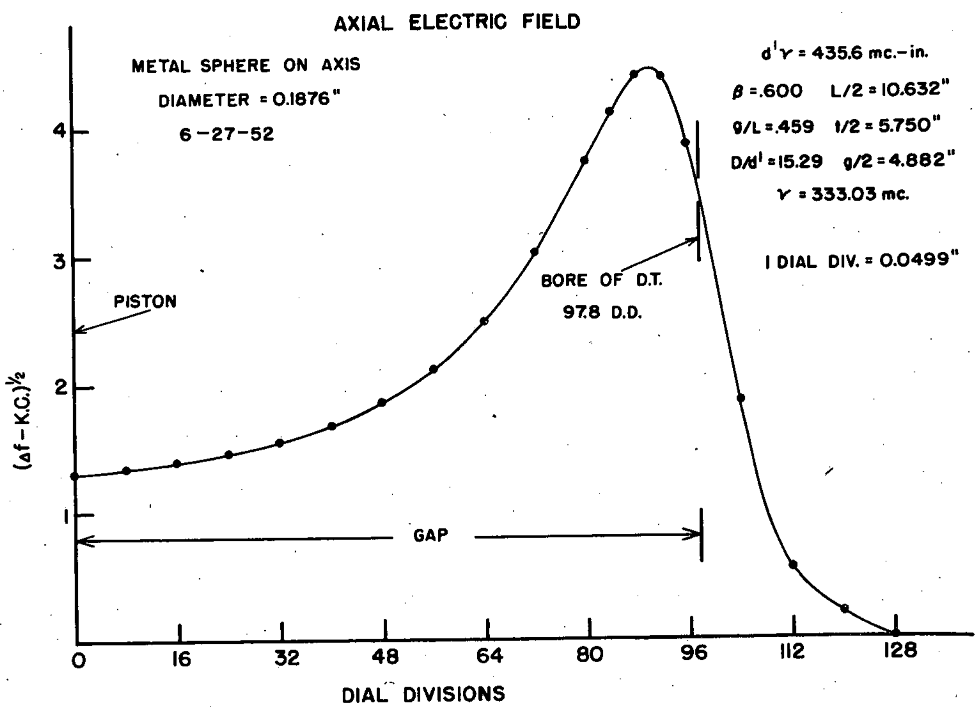

PIPE DRIFT TUBE FIELD DISTRIBUTION

FIG. 20a

MU-5065

MAGNETIC AND ELECTRIC FIELDS ALONG SURFACE OF PIPE D.T.

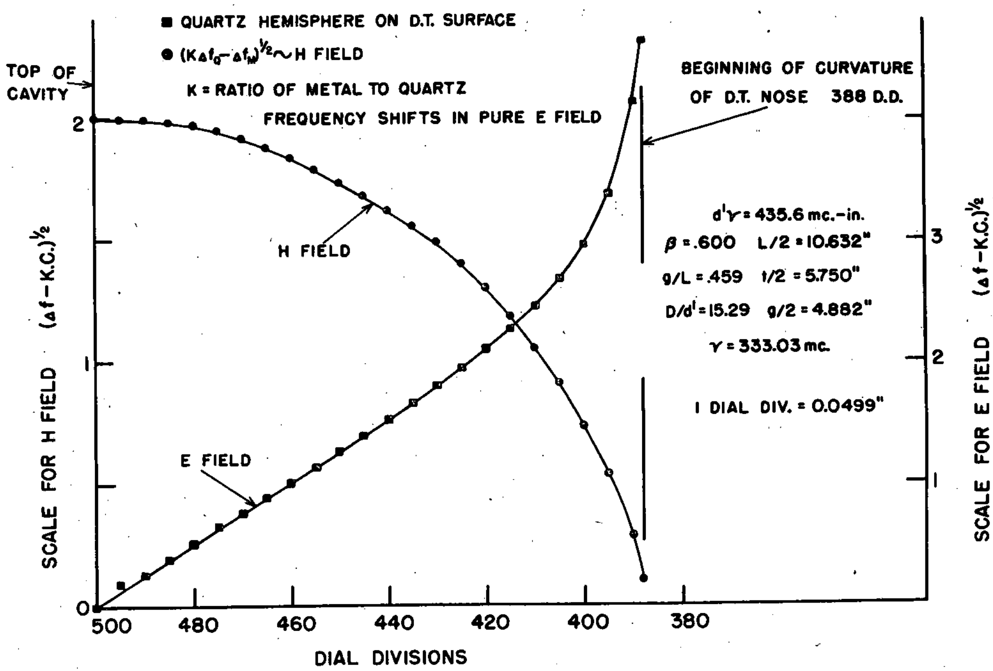

PIPE DRIFT TUBE FIELD DISTRIBUTION

MU-5066

Fig. 20b

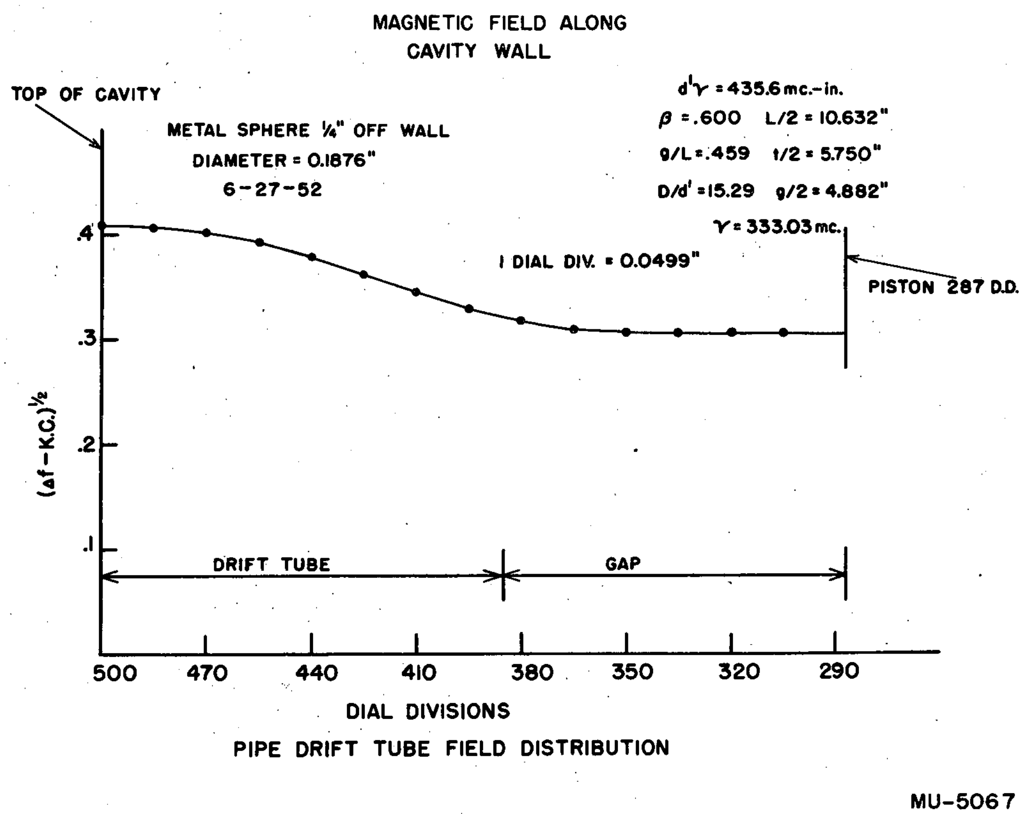
MAGNETIC FIELD ALONG
CAVITY WALL
TOP OF CAVITY
METAL SPHERE ¼" OFF WALL
DIAMETER = 0.1876"
6-27-52
d'γ = 435.6 mc.-in.
β = .600 L/2 = 10.632"
g/L = .459 t/2 = 5.750"
D/d' = 15.29 g/2 = 4.882"
γ = 333.03 mc.
1 DIAL DIV. = 0.0499"
PISTON 287 D.D.
(Δf-K.C.)½
.4
.3
.2
.1
DRIFT TUBE
GAP
500
470
440
410
380
350
320
290
DIAL DIVISIONS
PIPE DRIFT TUBE FIELD DISTRIBUTION
MU-5067

Fig. 20c

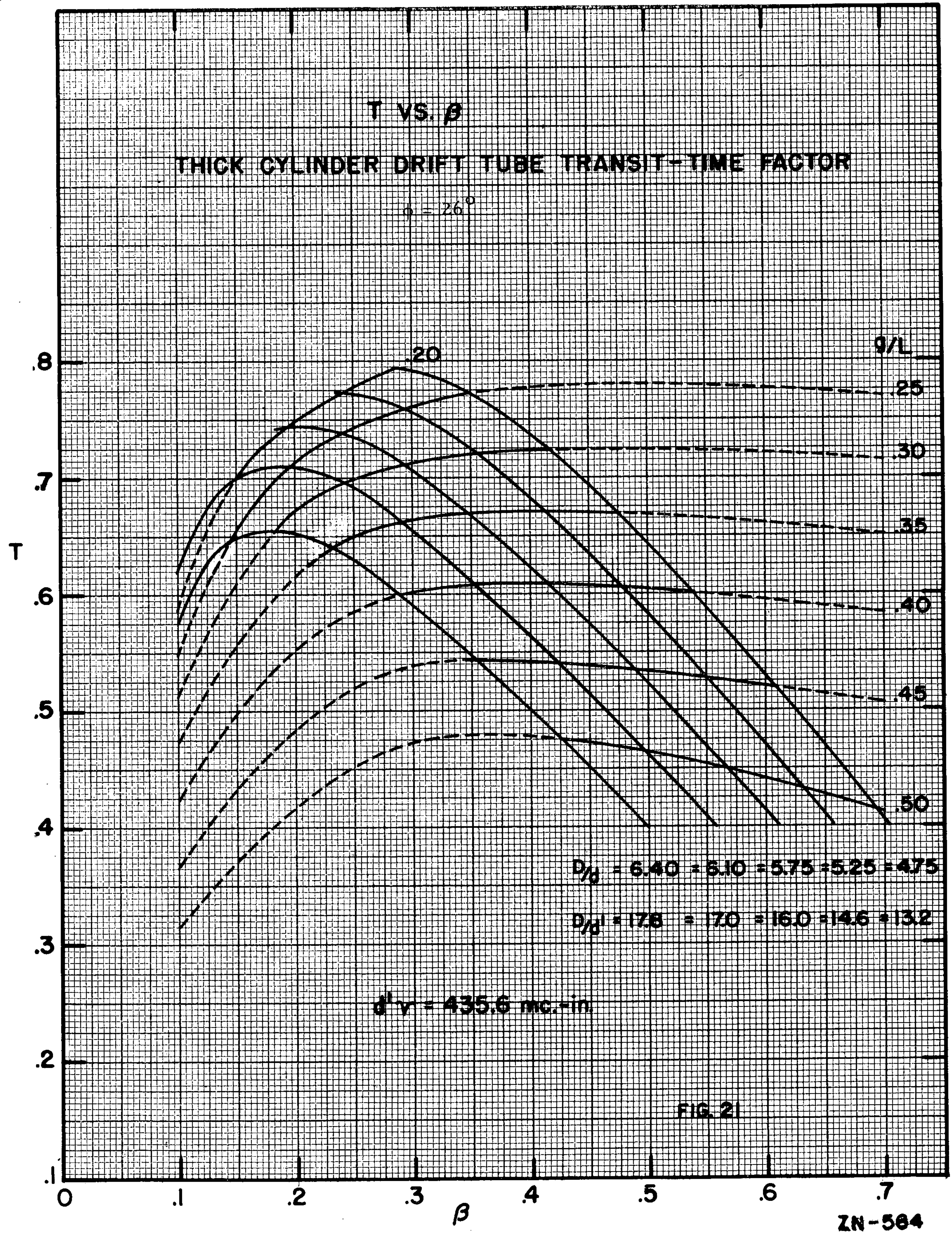
T VS. β
THICK CYLINDER DRIFT TUBE TRANSIT-TIME FACTOR
φ = 26°
g/L
.20
.25
.30
.35
.40
.45
.50
D/d = 6.40 = 6.10 = 5.75 = 5.25 = 4.75
D/d' = 17.8 = 17.0 = 16.0 = 14.6 = 13.2
d'ν = 435.6 mc.-in.
T
.8
.7
.6
.5
.4
.3
.2
.1
0
.1
.2
.3
.4
.5
.6
.7
β
FIG. 21

ZN-564

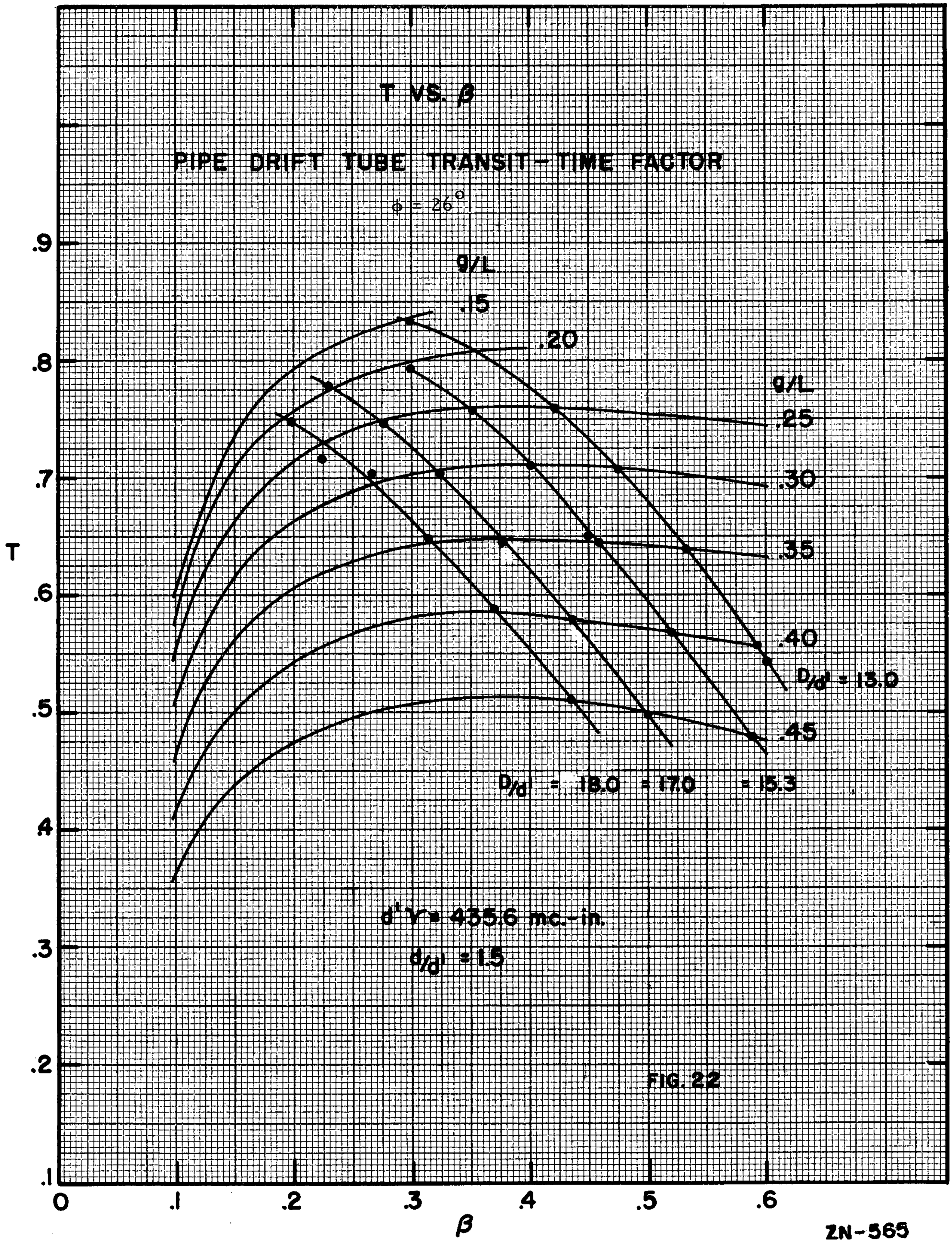
T VS. β
PIPE DRIFT TUBE TRANSIT-TIME FACTOR
φ = 26°
g/L
.15
.20
g/L
.25
.30
.35
.40
.45
D/d' = 13.0
D/d' = 18.0 = 17.0 = 15.3
d'ν = 435.6 mc.-in.
d/d' = 1.5
T
.9
.8
.7
.6
.5
.4
.3
.2
.1
0
.1
.2
.3
.4
.5
.6
β

FIG. 22

ZN-565

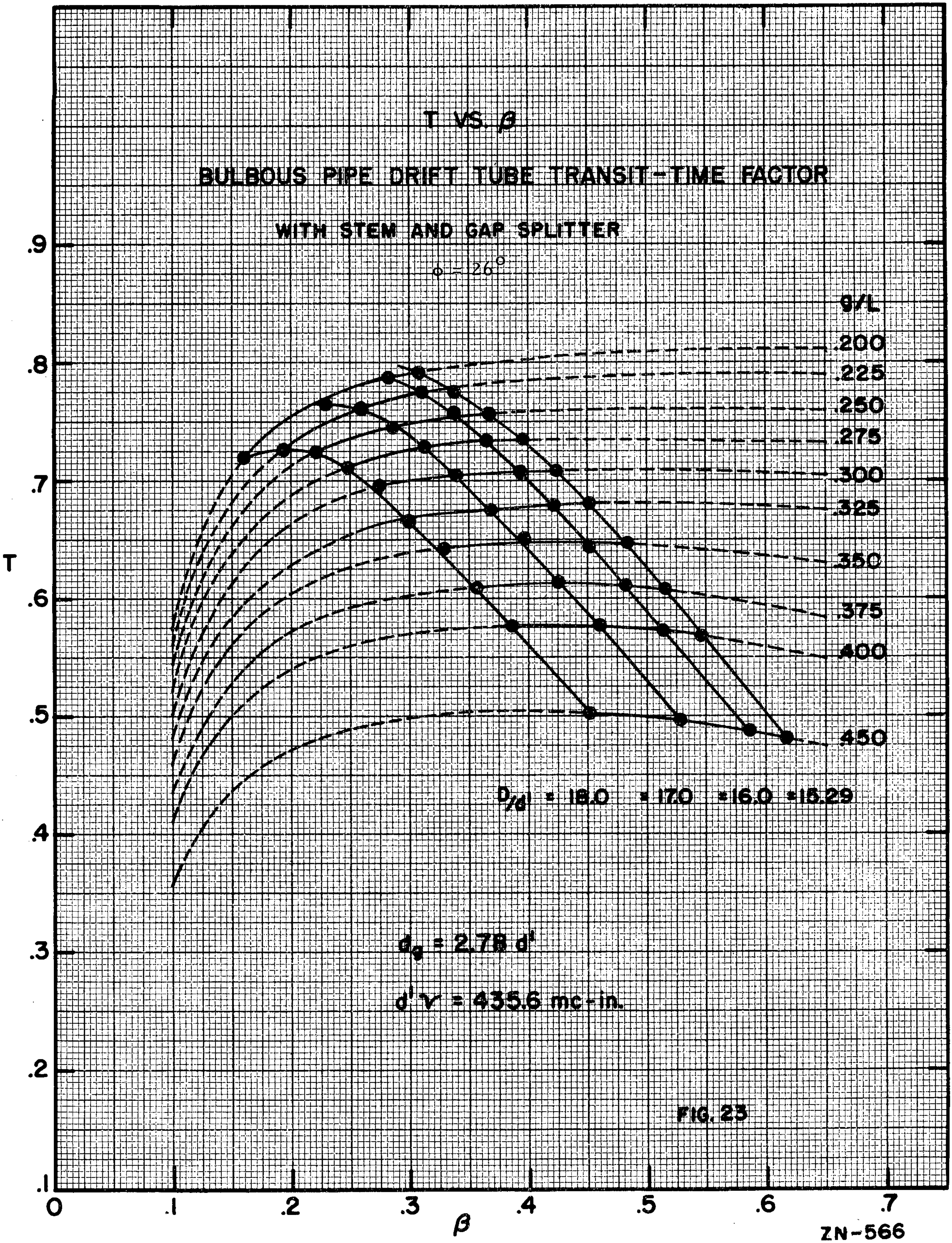
T VS. β
BULBOUS PIPE DRIFT TUBE TRANSIT-TIME FACTOR
WITH STEM AND GAP SPLITTER
φ = 26°
g/L
.200
.225
.250
.275
.300
.325
.350
.375
.400
.450
D/d' = 18.0 = 17.0 = 16.0 = 15.29
d_g = 2.78 d'
d'ν = 435.6 mc-in.
T
.9
.8
.7
.6
.5
.4
.3
.2
.1
0
.1
.2
.3
.4
.5
.6
.7
β

FIG. 23

ZN-566

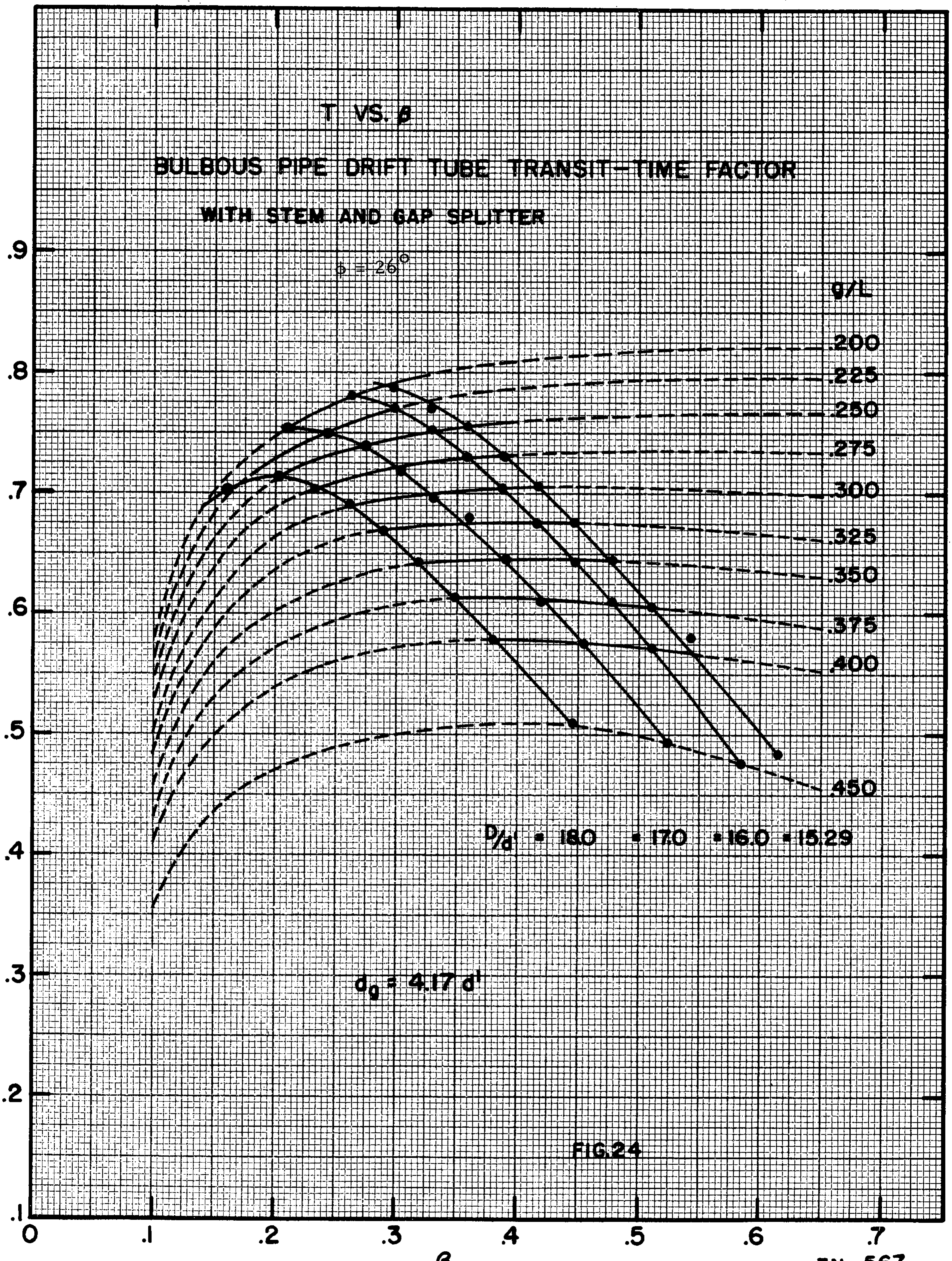
T VS. β
BULBOUS PIPE DRIFT TUBE TRANSIT-TIME FACTOR
WITH STEM AND GAP SPLITTER
φ = 26°
g/L
.200
.225
.250
.275
.300
.325
.350
.375
.400
.450
D/d' = 18.0 = 17.0 = 16.0 = 15.29
d_g = 4.17 d'
FIG.24
T
.9
.8
.7
.6
.5
.4
.3
.2
.1
0
.1
.2
.3
.4
.5
.6
.7
β

ZN-567

CONFIDENTIAL

DECLASSIFIED

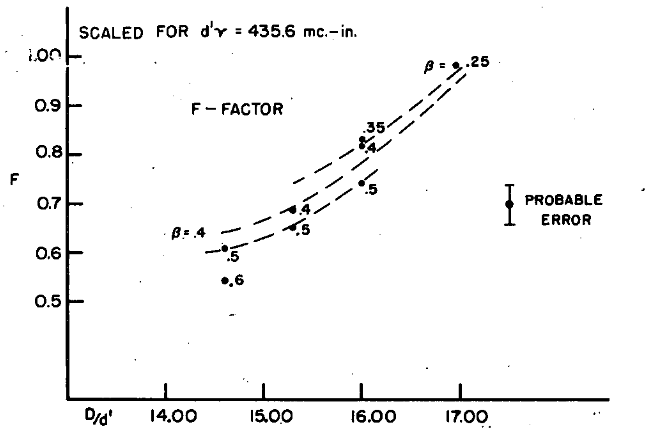

FIG. 25A. THICK CYLINDER DRIFT TUBE

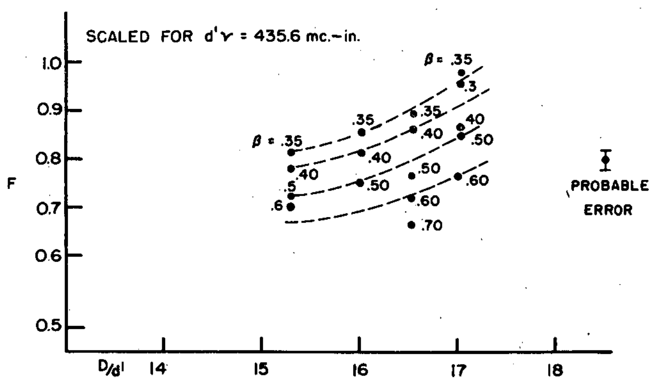

FIG. 25 b. PIPE DRIFT TUBE

DIMENSIONLESS SHUNT IMPEDANCE FACTOR

MU-5062

CONFIDENTIAL

CONFIDENTIAL

DECLASSIFIED

DECLASSIFIED

CONFIDENTIAL